Karlsruhe Institute of Technology

Evaluated data files for neutron irradiation of ^{182}W and ^{186}W at energies up to 200 MeV

by A.Yu. Konobeyev, U. Fischer, P.E. Pereslavtsev, S.P. Simakov

KIT SCIENTIFIC WORKING PAPERS 108

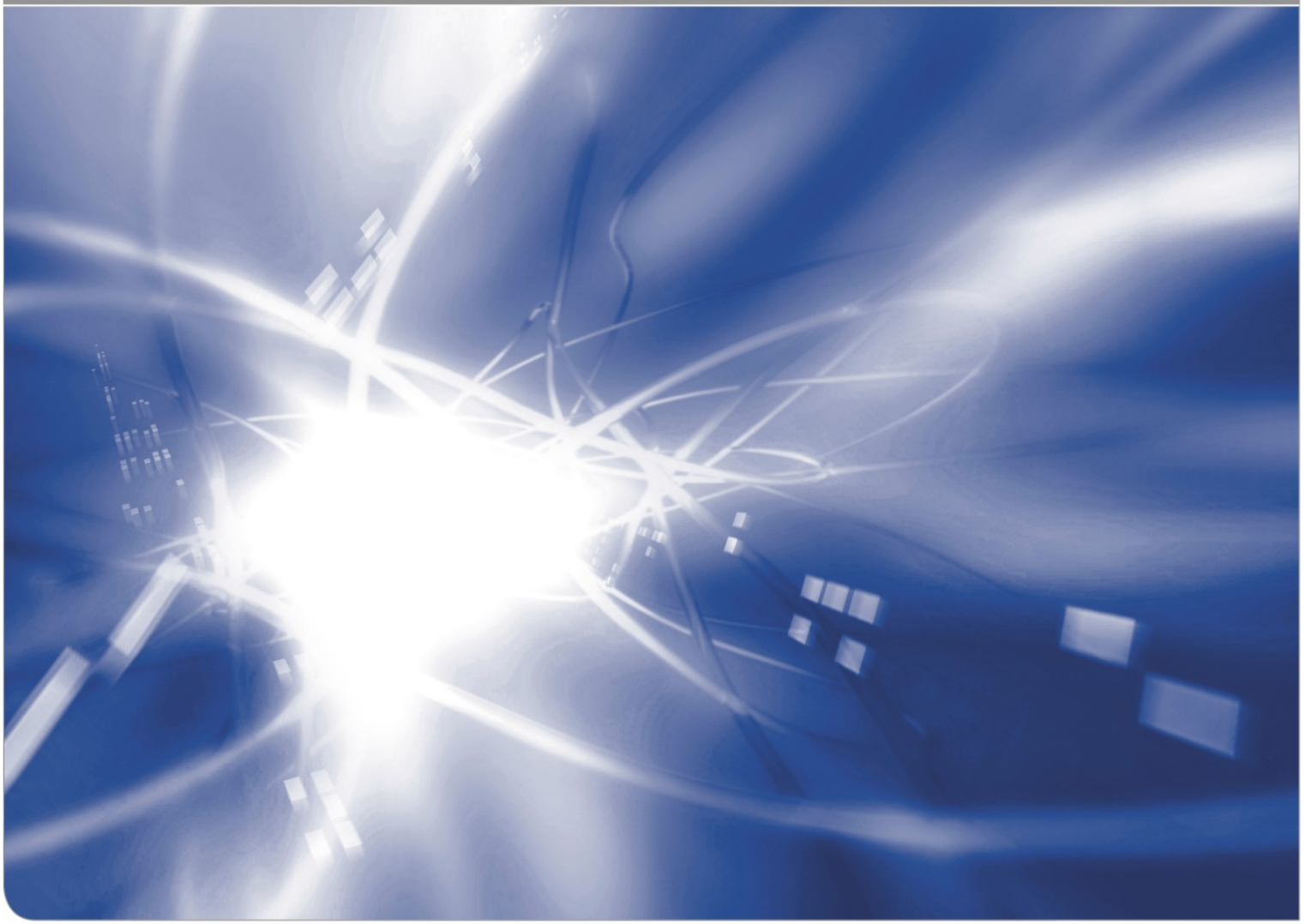

Institute for Neutron Physics and Reactor Technology, KIT

Impressum

Karlsruher Institut für Technologie (KIT)
www.kit.edu

2019

ISSN: 2194-1629

Abstract

New evaluated general purpose nuclear data files were prepared for ^{182,186}W isotopes at primary neutron energy up to 200 MeV. A special version of the TALYS code implementing the geometry dependent hybrid model (GDH) supplied with models for the non-equilibrium cluster emission was applied for calculations of nuclide production and particle energy distributions. The parameters of the GDH model were properly estimated using measured data for individual tungsten isotopes.

The evaluation of cross-sections was performed using results of model calculations, available experimental data, systematics of light charge particle production cross-sections, and obtained covariance information. The BEKED code package developed in KIT was used for numerical calculations. Data were formatted using the TEFAL code and the FOX code from BEKED.

CONTENTS

page

1. INTRODUCTION

Due to its unique properties, tungsten is a prime candidate for the first wall in fusion devices [1]. Reliable, high-quality evaluated data for tungsten are of particular importance for modelling neutron irradiation.

It has been more than ten years since evaluating data for tungsten isotopes in KIT [2]. The data are included in the JEFF-3.3 [3] and were successfully used for neutron transport calculations for fusion and fission reactors. Since then, calculation and evaluation methods have been further developed, and new experimental data have appeared.

The aim of this work was to use new information and advanced methods to obtain evaluated data for tungsten isotopes ^{182}W and ^{186}W irradiated with neutrons. The new data evaluation takes into account the experience of using previous data and provides both further improvement of the data quality concerning reliability and completeness. The calculation of nuclide production cross-sections and particle energy distributions was performed using a special version of the TALYS code [4-7] providing calculations with geometry dependent hybrid model [8-11].

Section 2 describes the evaluation procedure concerning nuclear model calculations, use of experimental data, combination of results of calculations and measurements, and recording the file with evaluated data. Section 3 discusses evaluated data for ^{182}W and Section 4, data for ^{186}W.

2. EVALUATION PROCEDURE

The evaluation consists of following steps: i) the calculation of cross-sections, angular distributions for elastic scattering, energy distributions of emitted particles, and the calculation of covariance matrices for cross-sections, ii) the processing obtained data in a file in the ENDF-6 format [12], iii) the selection and analysis of experimental data for subsequent combination with results of calculations, iv) the evaluation using experimental data, results of model calculations, and covariance information, v) the recording final data in the ENDF-6 format, and vi) the general check of evaluated data file.

The steps are briefly discussed below.

2.1 Calculations using nuclear models

The special version of the TALYS code [5,7] implementing Blann's geometry dependent hybrid model (GDH) [9] and supplied with models for the non-equilibrium cluster emission [11,6] was applied for calculations of nuclear reaction cross-sections and particle energy distributions. The parameters of the GDH model were properly estimated using available measured data [7]. The discussion can be found in Refs.[6,7].

According to the GDH model the energy distribution of precompound nucleons is calculated as follows [9]:

$$\frac{d\sigma}{d\varepsilon_x} = \pi\lambda\!\!\!^{-2} \sum_{l=0}^{\infty} (2l+1) T_l \sum_{n=n_0} {}_nX_x \frac{\omega(p-1,h,U)}{\omega(p,h,E)} \frac{\lambda_x^e}{\lambda_x^e + \lambda_x^+} g D_n , \qquad (1)$$

where T_l is the transmission coefficient for l-th partial wave; ${}_nX_x$ is the number of nucleons of type "x" in the n-exciton state; ε_x is the channel energy of the nucleon; $\omega(p,h,E)$ is the density of exciton states with "p" particles and "h" holes ($p+h=n$) at the excitation energy E; U is the final excitation energy, g is the single particle level density, D_n is the factor [10], which takes into account a "depletion" of the n-exciton state due to the nucleon emission; n_0 is the initial exciton number.

The nucleon emission rate λ_x^e is equal to

$$\lambda_x^e = \frac{(2S_x+1)\mu_x \varepsilon_x \sigma_x^{inv}(\varepsilon_x)}{\pi^2 \hbar^3 g_x} , \qquad (2)$$

where common designations are used.

The intranuclear transition rate λ_x^+ is defined as follows

$$\lambda_x^+ = V \sigma_0(\varepsilon_x) \rho_l , \qquad (3)$$

where V is a velocity of a nucleon inside the nucleus, σ_0 is the nucleon-nucleon scattering cross-section corrected for the Pauli principle [9], ρ_l is the average nuclear matter density at the distance from $l\lambda\!\!\!^{-}$ to $(l+1)\lambda\!\!\!^{-}$.

The energy distributions of pre-equilibrium deuterons, tritons, ^{3}He-nuclei, and α-particles are calculated as a sum of components concerning pick-up, knock-out, and direct processes. Details are discussed in Refs.[11,6,7].

The GDH calculations are selected with the input parameter *preeqmode* equal to five.

An extensive comparison of model predictions with experimental data is can be found in Ref.[7].

The total cross-section, elastic cross-section, elastic angular distribution, and contribution of direct processes in inelastic scattering were calculated using the ECIS-06 code [13] integrated in the TALYS code [5].

The equilibrium particle emission was simulated using the Hauser-Feshbach model [4,5,14]. The Fermi gas model with the energy dependent level density parameter [15] combined with the “constant temperature” model [4,5,16] was applied for nuclear level density calculations.

The covariance matrices for cross-sections were calculated using the Monte Carlo method proposed in Ref.[17]. The calculations consists of following steps: the choice of the “best” set of parameters for selected nuclear models, the assessment of uncertainties of model parameters, the Monte Carlo sampling of N number of input data sets, the execution of calculations for obtained input data files, and the calculation of covariance matrices for particular reactions

$$V_{ij} = N^{-1} \sum_{k=1}^{N} (\sigma_{ik} - \sigma_{i0})(\sigma_{jk} - \sigma_{j0}) \qquad (4)$$

where σ_{ik} is the cross-section corresponding to the “*i*”-th primary neutron energy in the “*k*”-th Monte Carlo event, σ_{i0} is the cross-section obtained using the “best“ set of model parameters.

2.2 Processing of output data

Processing of TALYS output information and recording of preliminary data file in the ENDF-6 format was performed using the TEFAL-1.9 code [18,19]. The code collects TALYS output data files prepared with the input option “*endf y*”.

At this stage, the resonance parameters from JEFF-3.3 were included in the file.

2.3 Use of experimental data

Experimental data for ^{182}W and ^{186}W were taken from Refs.[20-85], cited by information recorded in EXFOR [86]. Data from EXFOR were converted to C4 format [87] for further use. In some cases, errors of cross-sections, automatically selected by processing, were specified using available information.

The ENSDF data [88] were used for the analysis of measurements of (n,n') reaction cross-sections in Refs.[34,52].

2.4 Cross-section evaluation

The evaluation of cross-sections using experimental data, results of model calculations, and covariance information was performed using the generalized least-squares method [89]. The BEKED package [90] was applied for numerical computations. Examples of evaluated cross-sections are given in Section 3 and 4.

2.5 Recording data in ENDF-6 format

Evaluated data were consistently integrated in the final data file.

Even a relative small change in the cross-section for a specific reaction after the evaluation comparing to calculated value results to specific changes in the final data file: change of the contribution of isomers (MF=9,10), absorption cross section (MF/MT=3/3), total cross section, sum of cross sections recorded in MF/MT= 3/5, the production cross section for corresponding residual nucleus in MF/MT= 6/5, the yields for all residuals recorded in the MF/MT= 6/5, including neutron production, gas-production components, and γ-production due to the change in MF/MT= 3/5. Such re-calculations and corrections of data are performed using the FOX code from BEKED. Special attention is paid to avoiding jumps in cross sections values at the transition from MF=3 to MF/MT=6/5 data representation.

Checking the obtained file before processing with NJOY [91] is carried out using checking codes [92] and the COVEIG code [93].

3. DATA OBTAINED FOR ^{182}W

In this Section evaluated data for ^{182}W are compared with data from other libraries, experimental data, systematics data, and calculations.

Data from following evaluated data libraries are plotted in figures below, where appropriate: EAF-2010 [94], JENDL-4.0 [95], JENDL-4/HE [96], JENDL/AD-2017 [97], JENDL-HE [98], ENDF/B-VIII [99], TENDL-2017 [18,100], and JEFF-3.3 [3].

3.1 Total and elastic cross-section

Evaluated total and elastic cross-sections are shown in Fig.1 and Fig.2 together with measured data, and evaluated data from different libraries. A reasonable agreement is observed between obtained cross-sections and experimental data.

In general, evaluated cross-sections and data from libraries are close at energies below 1 MeV and above 15 MeV. Most of the data, including present evaluation, agree with measurements [25] at high energies. Since the elastic scattering cross sections from data libraries do not differ significantly (Fig.2), the discrepancy of total cross-sections at neutron energies between 1 and 15 MeV is due to different absorption cross-sections. In Fig.2, data from JENDL-4/HE are almost invisible at energies below 20 MeV, since TENDL-2017 cross-sections are close to these values.

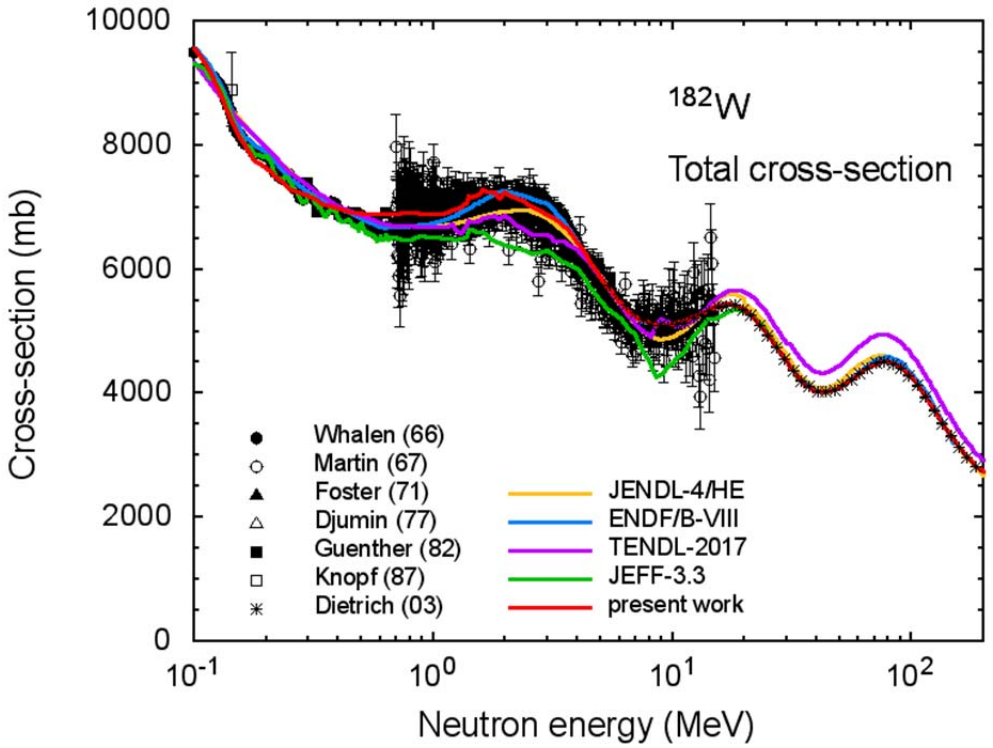

Fig.1 The total reaction cross-section for neutron irradiation of ^{182}W evaluated in the present work, measured data, and data taken from different libraries.

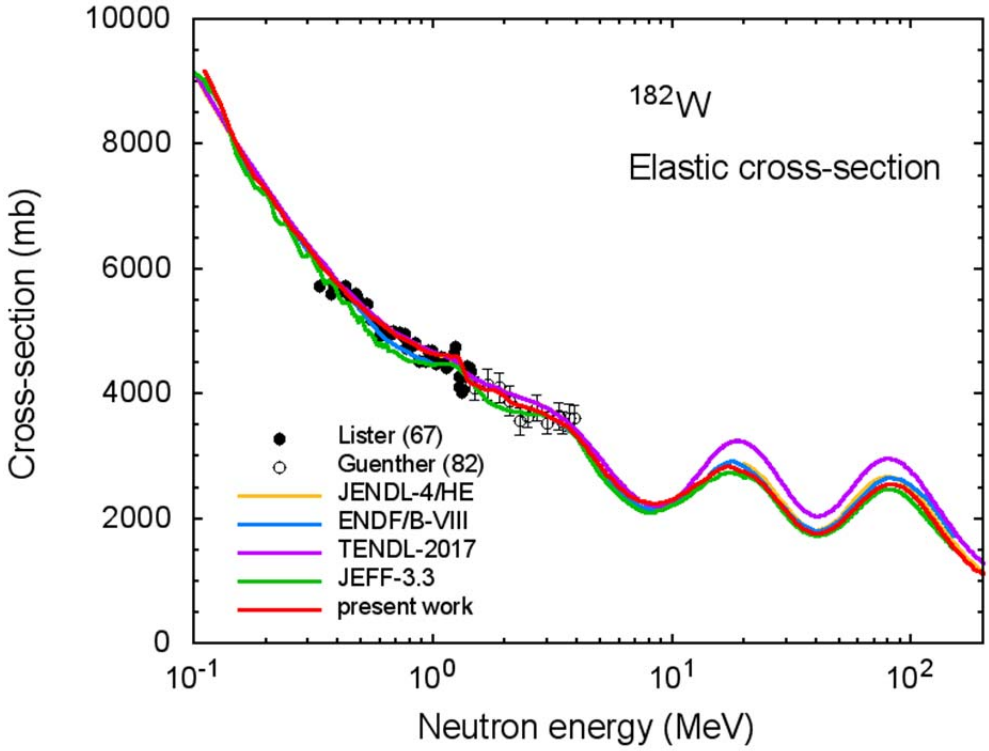

Fig.2 The cross-section for elastic neutron scattering for ^{182}W evaluated in the present work, measured data, and data taken from different libraries.

3.2 Inelastic scattering

Figures 3-5 show cross-sections for inelastic neutron scattering with excitation of the first three levels of ^{182}W. The corresponding data are recorded in the ENDF file in sections with MT- numbers from 51 to 53.

The cross-sections obtained for the first two levels, 0.1001 MeV (2^+) and 0.3294 MeV (4^+) (Figs.3,4) are consistent with measurements and data from other libraries. For the level 0.6804 MeV (6^+) (Fig.5), evaluated data are somewhat lower than experimental ones.

3.3 Various reactions

Figures 6-15 show evaluated cross sections for different nuclear reactions for n+ ^{182}W irradiation. In general, data obtained agree with experimental data.

The difference between evaluated (n,γ) reaction cross-section and the data from other libraries is observed in the energy region, where experimental data are not available (Fig.6).

The evaluated (n,2n) reaction cross-sections (Fig.7) are close to experimental data from Ref.[32] and differ somewhat from data of other libraries. Cross sections obtained for the ^{182}W(n,nα)^{178m2}Hf reaction are close to JENDL/AD-2017 data and are quite different from calculated cross sections (Section 2.1) and cross-sections from TENDL-2017 and EAF-2010 (Figs.8,9). The same can be said about the ^{182}W(n,α)^{179m2}Hf reaction (Figs.14,15). For the (n,p) reaction, a relative agreement is observed for evaluated cross-sections and data from other sources (Figs.10,11). At the same time, obtained (n,α) reaction cross-sections and other data differ at energies above 14 MeV (Figs.12,13).

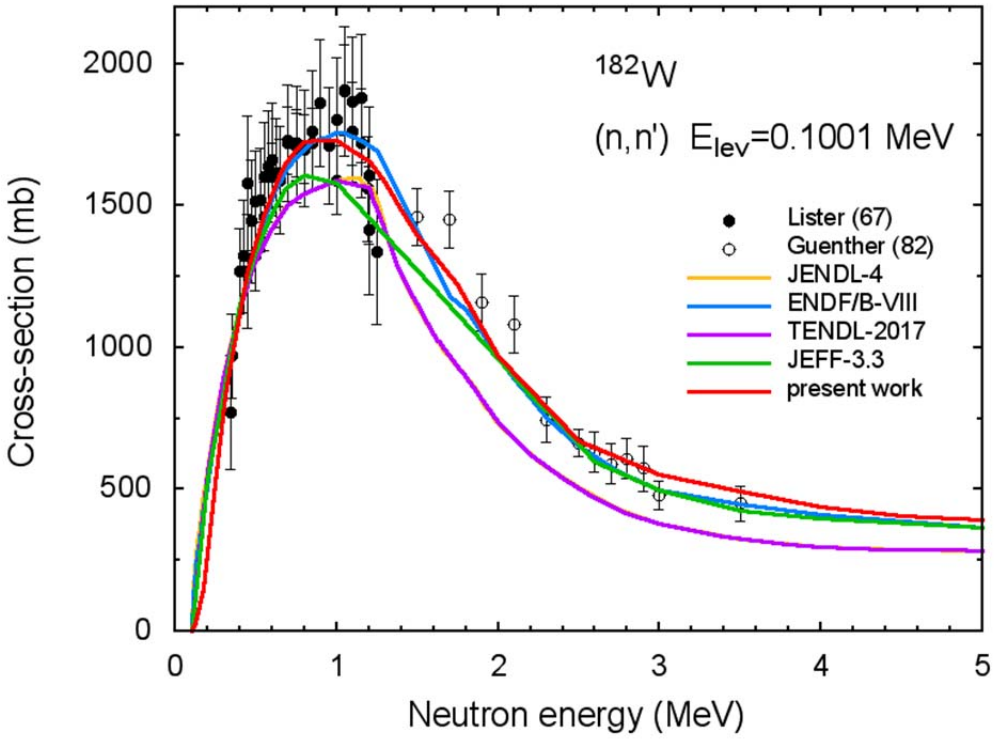

Fig.3 The inelastic scattering cross-section ^{182}W(n,n') with excitation of the first level 0.1001 MeV (2^+).

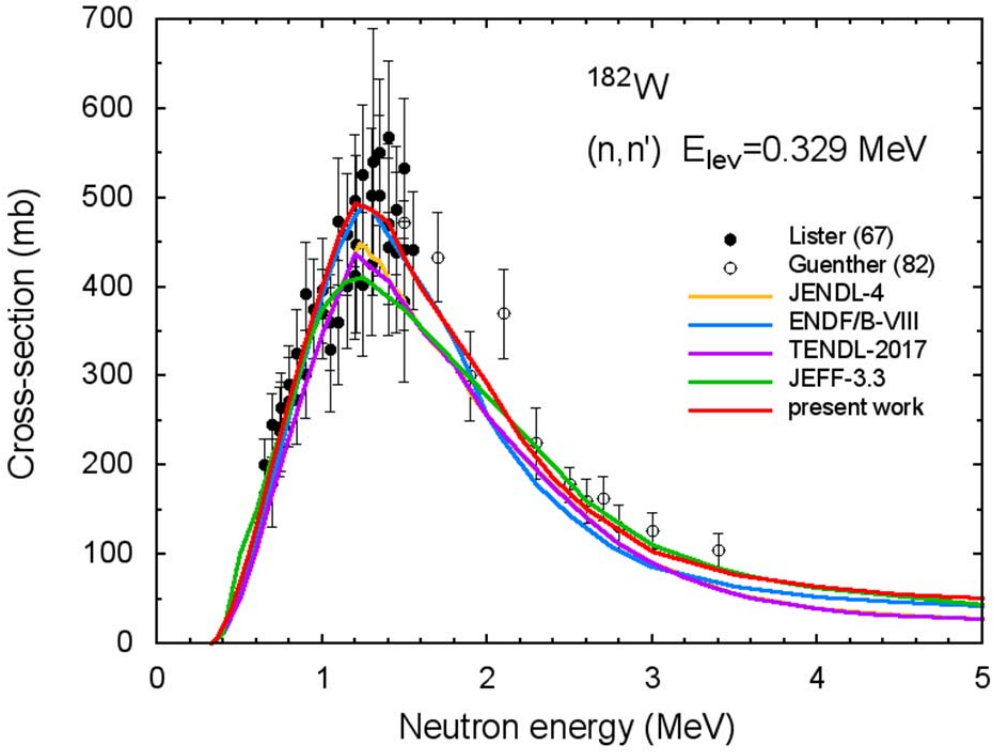

Fig.4 The inelastic scattering cross-section ^{182}W(n,n') with excitation of the second level 0.3294 MeV (4^+).

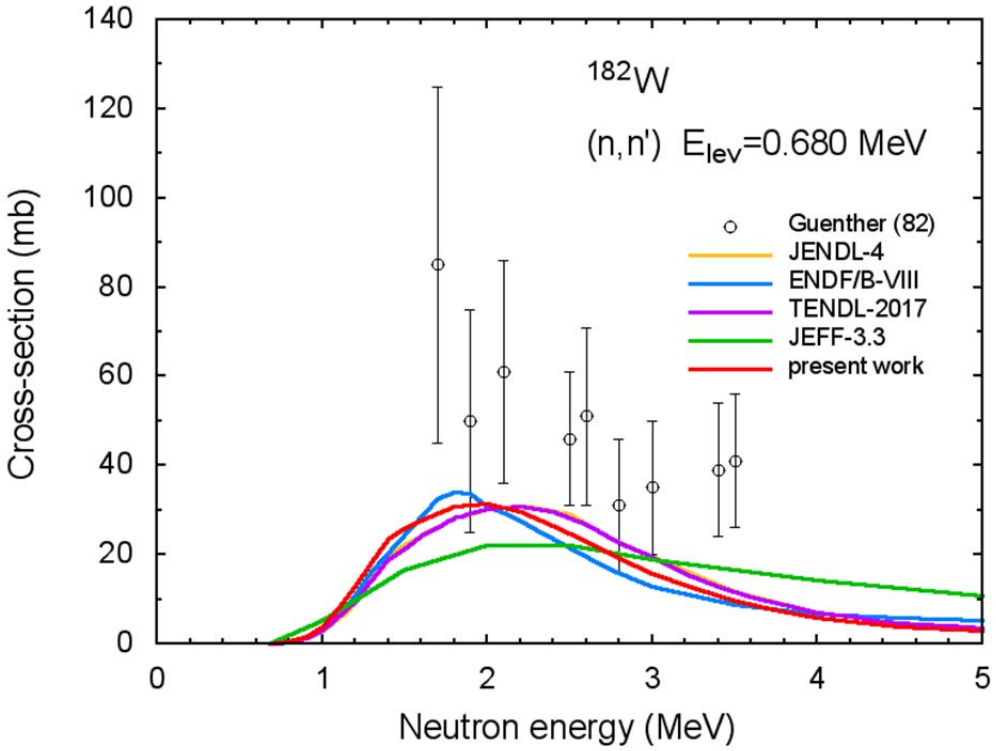

Fig.5 The inelastic scattering cross-section ^{182}W(n,n') with excitation of the third level 0.6804 MeV (6^+).

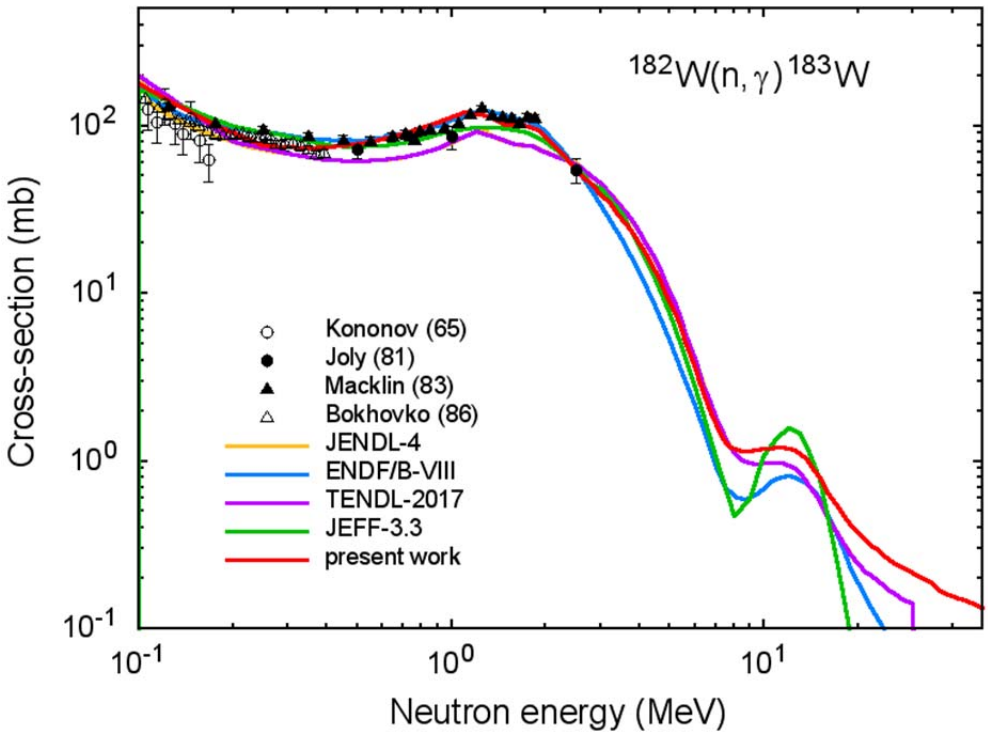

Fig.6 The (n,γ) reaction cross-section for ^{182}W.

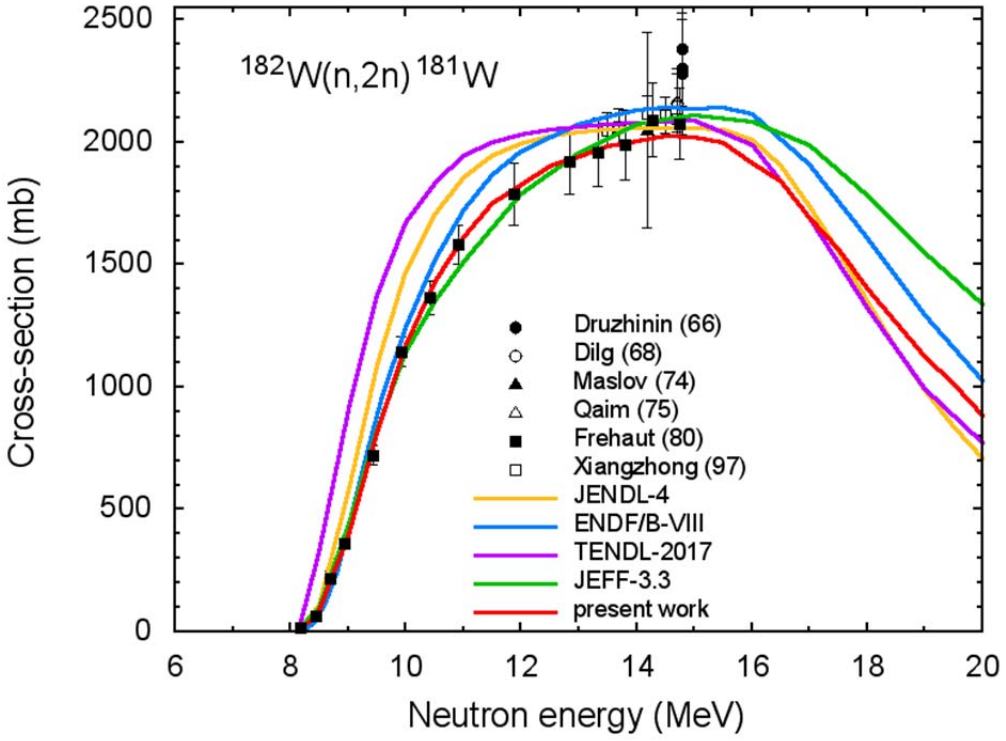

Fig.7 The (n,2n) reaction cross-section for ^{182}W.

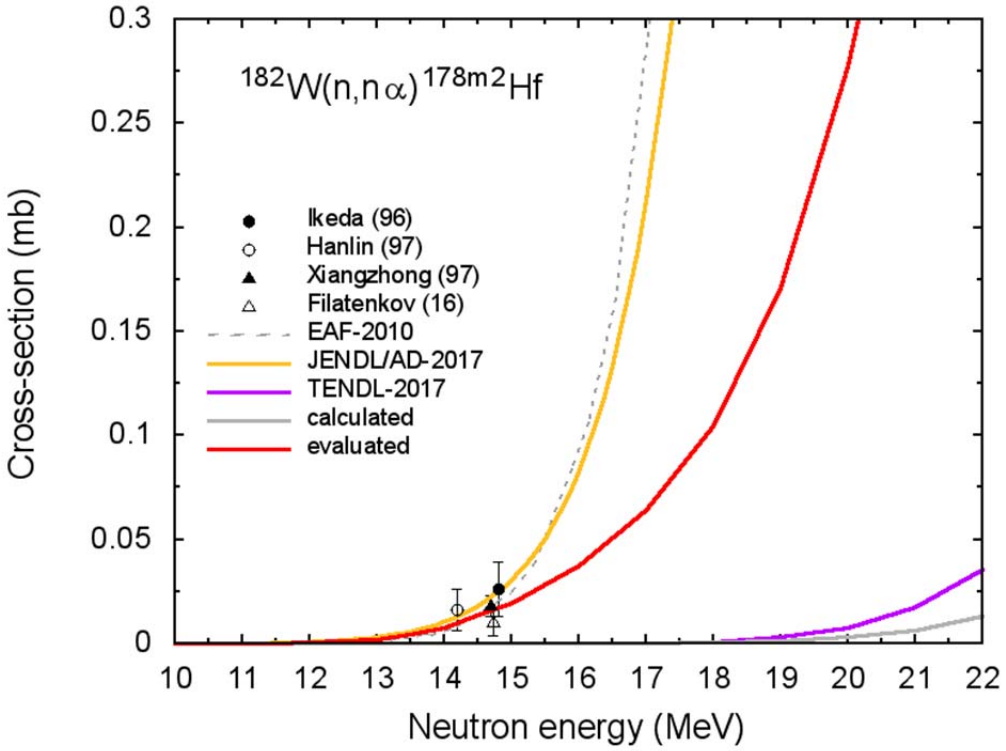

Fig.8 The $^{182}W(n,n\alpha)^{178m2}Hf$ reaction cross-section.

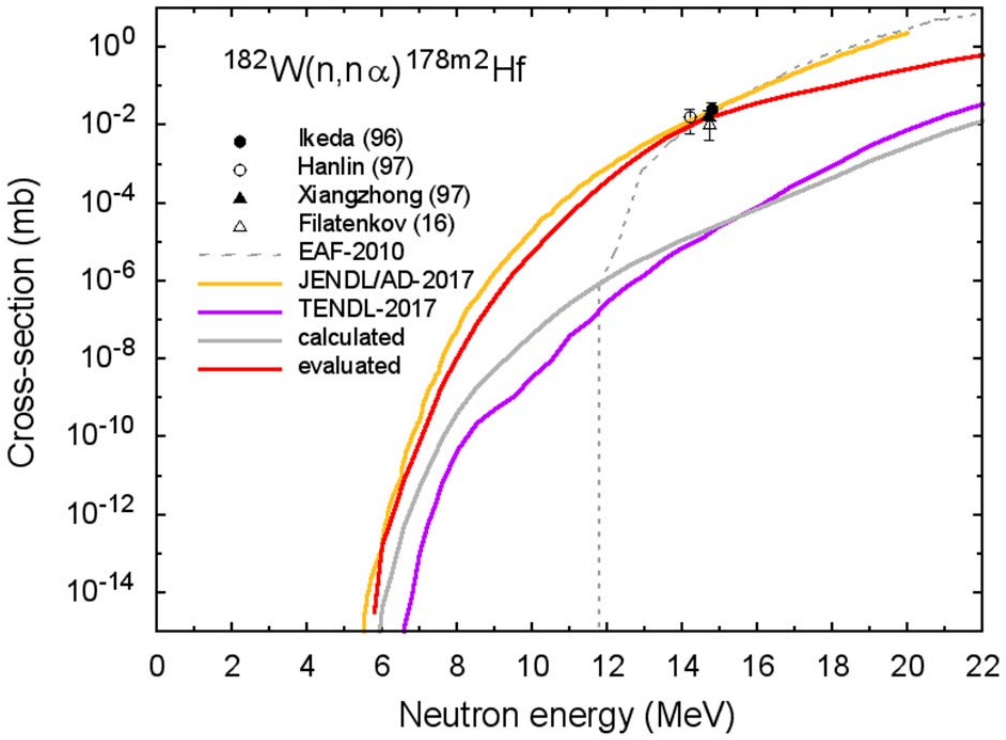

Fig.9 The same as in Fig.8, but on a logarithmic scale.

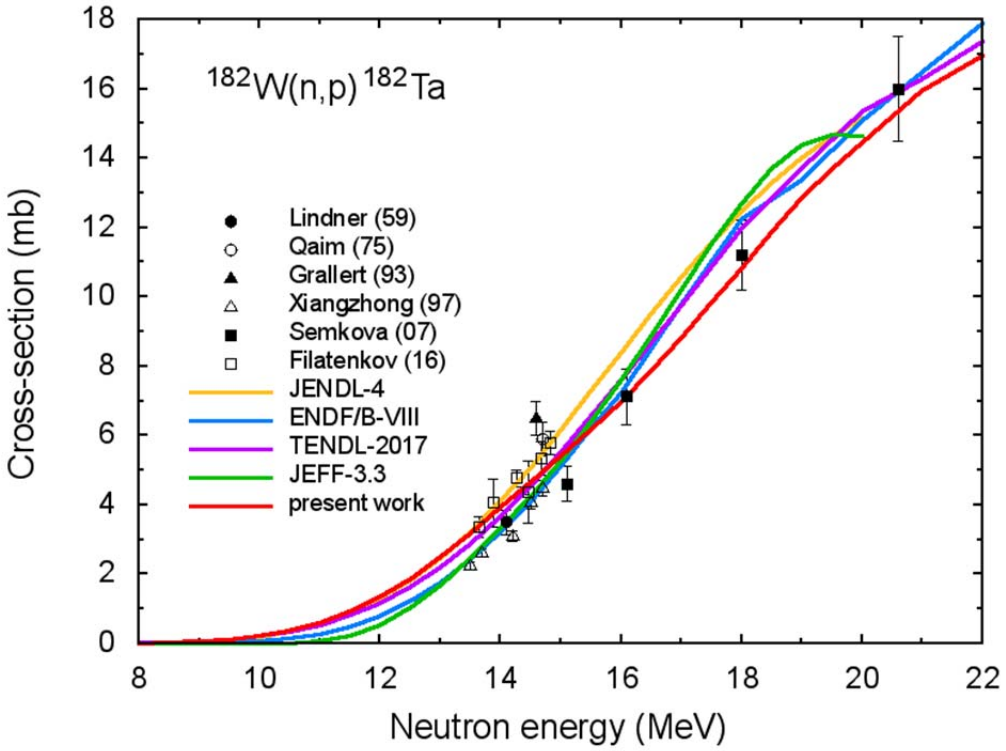

Fig.10 The (n,p) reaction cross-section for ^{182}W.

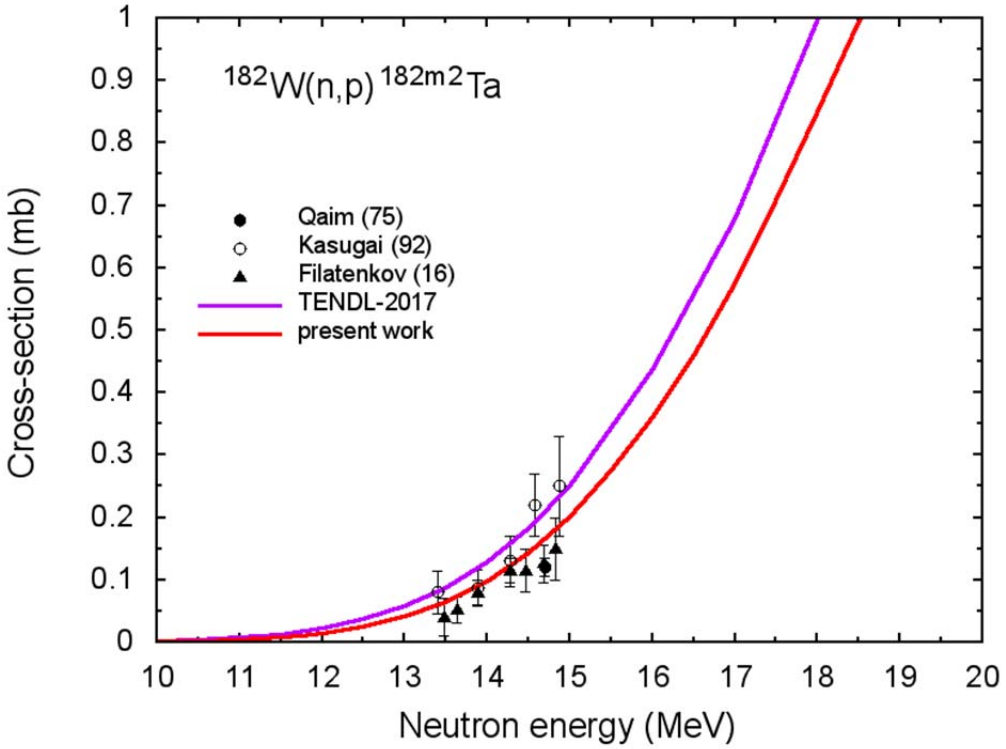

Fig.11 The ^{182}W(n,p)^{178m2}Ta reaction cross-section.

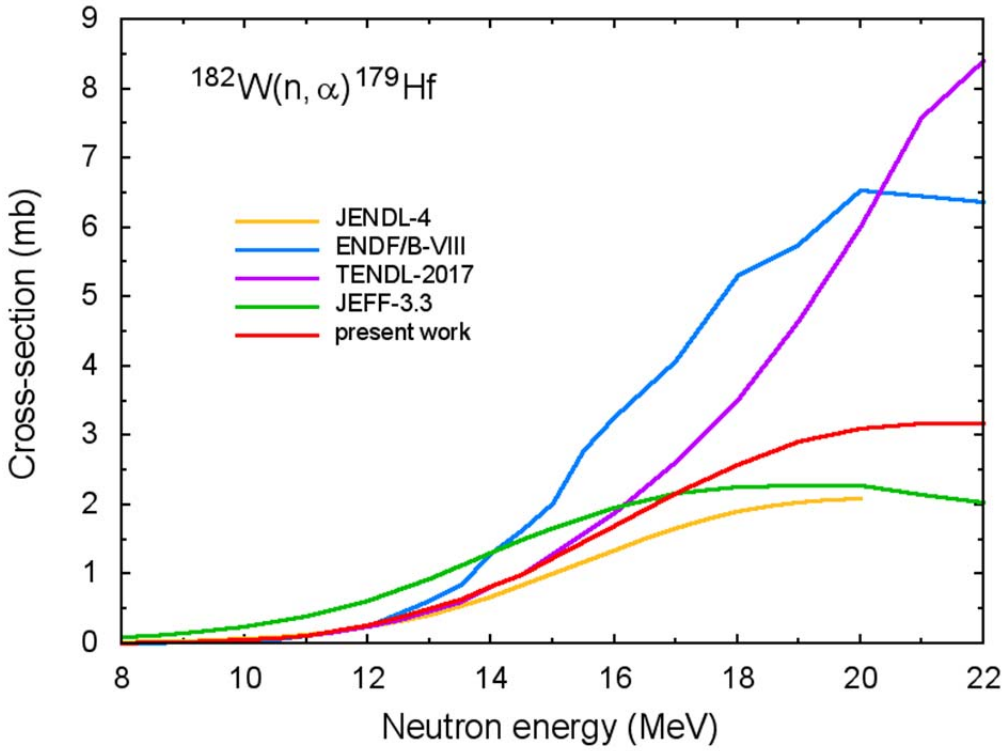

Fig.12 The (n,α) reaction cross-section for ^{182}W.

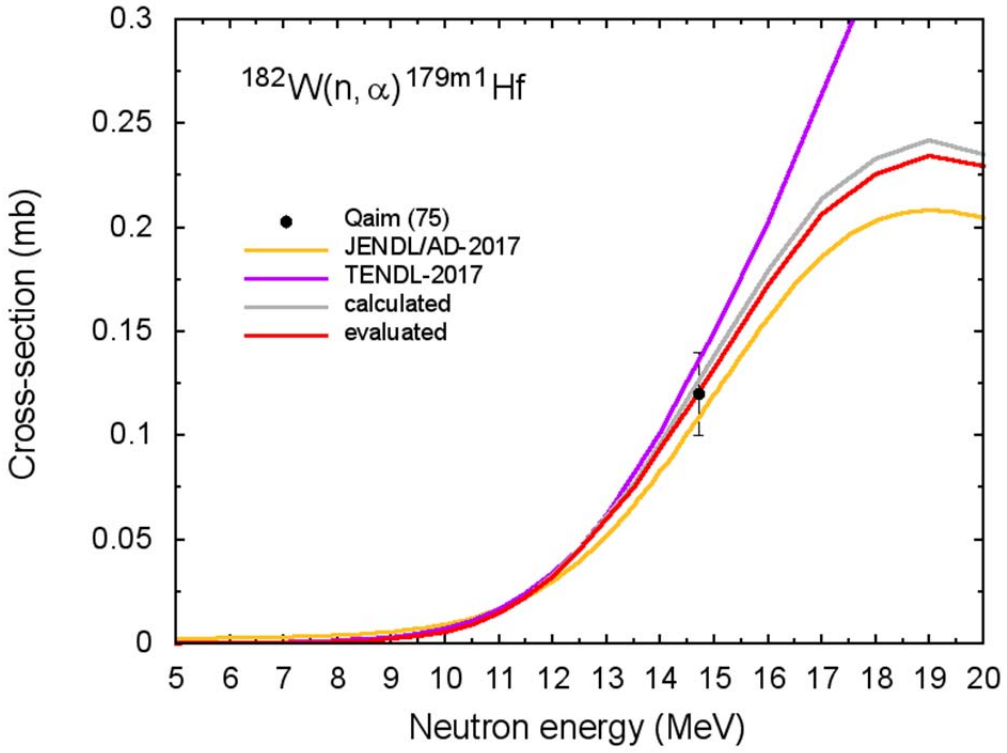

Fig.13 The ^{182}W(n,α)^{179m1}Hf reaction cross-section.

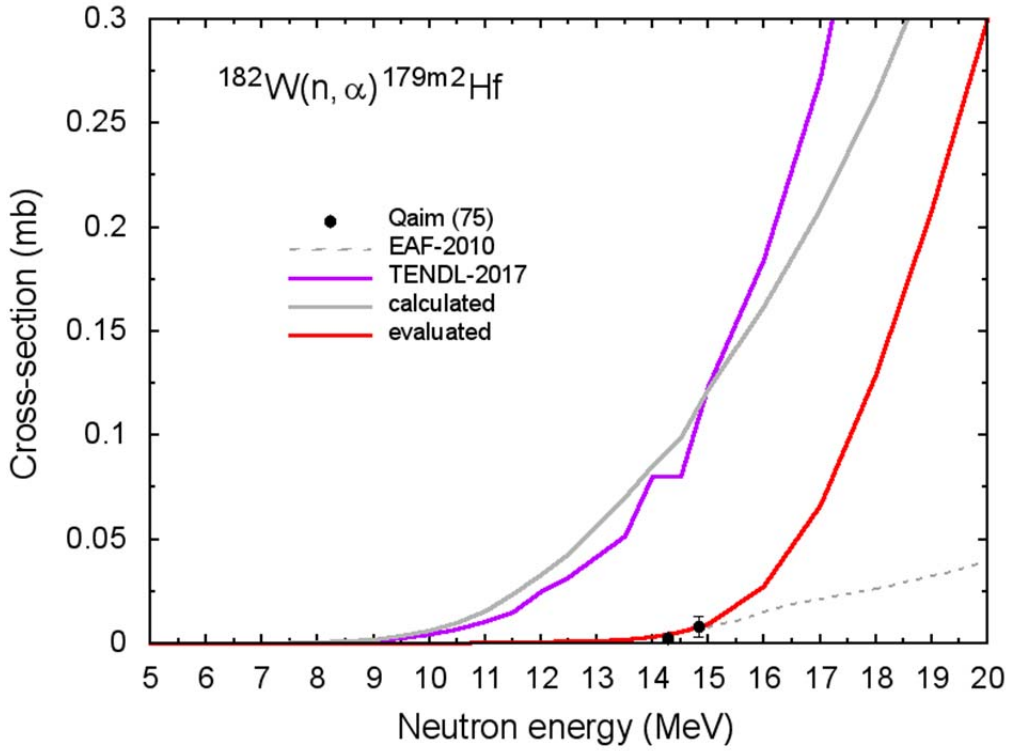

Fig.14 The ^{182}W(n,α)^{179m2}Hf reaction cross-section.

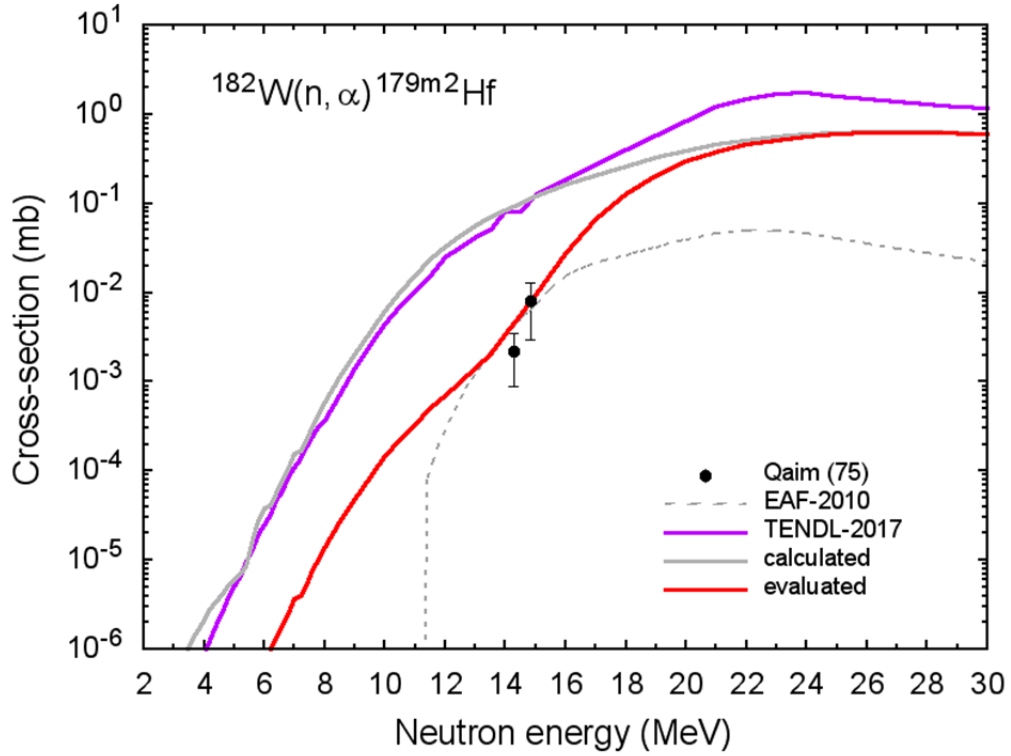

Fig.15 The same as in Fig.14, but on a logarithmic scale.

3.4 Neutron energy distribution

Measurements of neutron energy distributions are absent for ^{182}W. The comparison of the neutron spectrum for ^{182}W with the available experimental data for the natural mixture of tungsten isotopes (Fig.16) is rather conditional and can be used to illustrate the general agreement of the data rather than verify absolute values.

The neutron spectra from different libraries for a primary energy of 14.1 MeV are compared in Fig.17. Most of the evaluated curves have similar energy dependence.

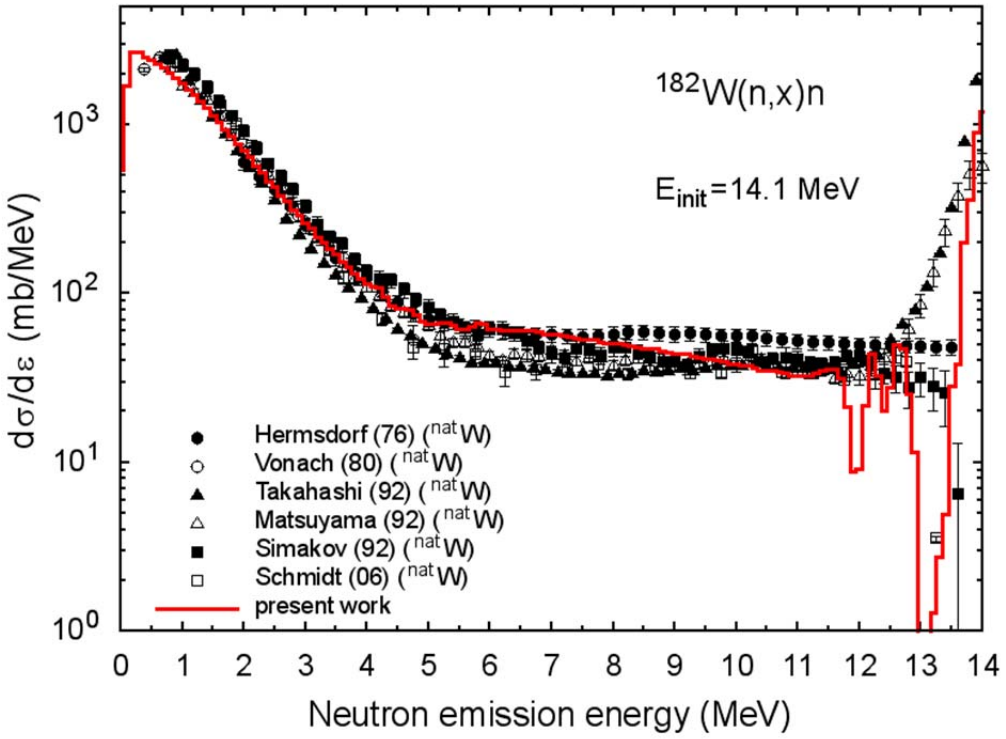

Fig.16 The neutron energy distributions in ^{182}W(n,x)n reaction induced by 14.1 neutrons obtained in the present work and measured for natural mixture of tungsten isotopes.

3.5 Light particle production cross-sections

Figures 18-28 show cross sections for the generation of neutrons in n+^{182}W reaction and components of gas production cross sections, consisting of proton- deuteron-, triton-, ^{3}He-, and α-particle formation cross-sections.

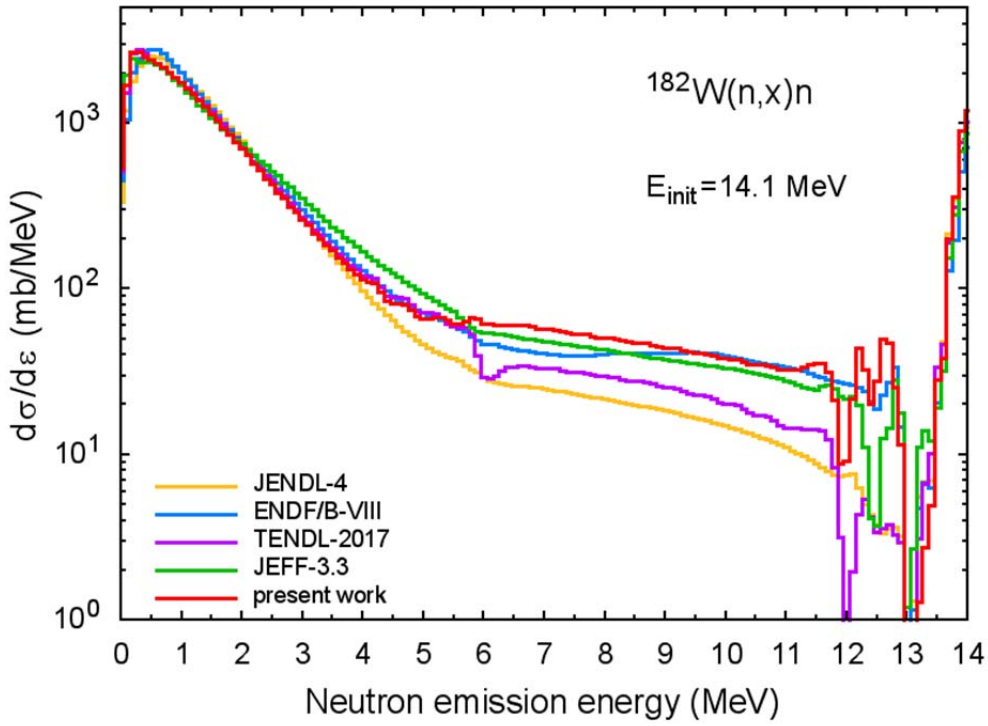

Fig.17 The neutron energy distributions in ^{182}W(n,x)n reaction induced by 14.1 MeV neutrons obtained in the present work and taken from various data libraries.

To illustrate the consistency of the obtained integrated (n,xn) cross sections with high-energy calculations, Fig.18 shows the neutron production cross-section calculated using the intranuclear cascade evaporation model applying the CASCADE code [101,102] and CEM03 code [103,104]. The energy dependence of cross sections obtained in the present work generally agrees with calculations using high-energy models.

Obtained cross-sections for light charged particle formation are compared with data from other libraries and the “reference” data in Figs. 19-28. The “reference” data were obtained in Refs.[105,106] as the result of the evaluation of the atomic mass number (A) dependency of investigated cross sections at fixed incident energy, by analogy with the usual evaluation of the energy dependence of cross sections for a fixed nucleus. For this purpose, available experimental data and results of calculations using different nuclear models have been applied in Refs.[105,106].

For a better illustration, the cross sections for the production of light charged particles are shown on two scales: linear (Figs.19,21,23,25,27) and logarithmic (Figs.20,22,24,26,28). In general, the energy dependence of obtained cross sections (Figs.19-28) seems reasonable, and the absolute values are consistent with the estimated data [105,106].

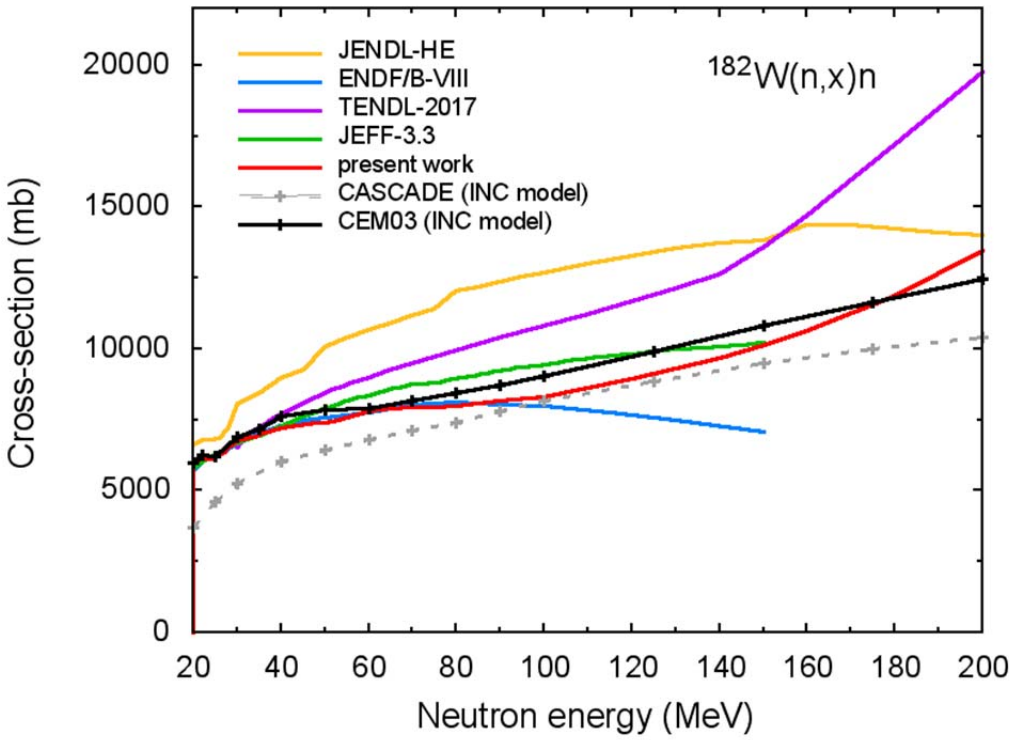

Fig.18 The neutron production cross-section for ^{182}W.

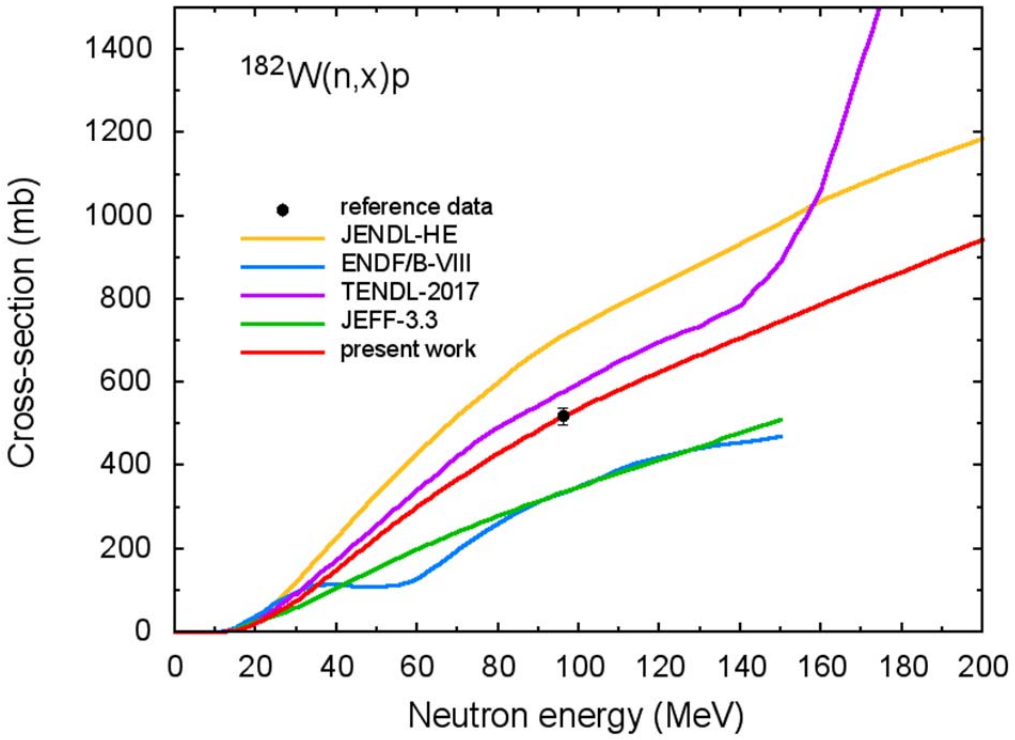

Fig.19 The proton production cross-section for ^{182}W.

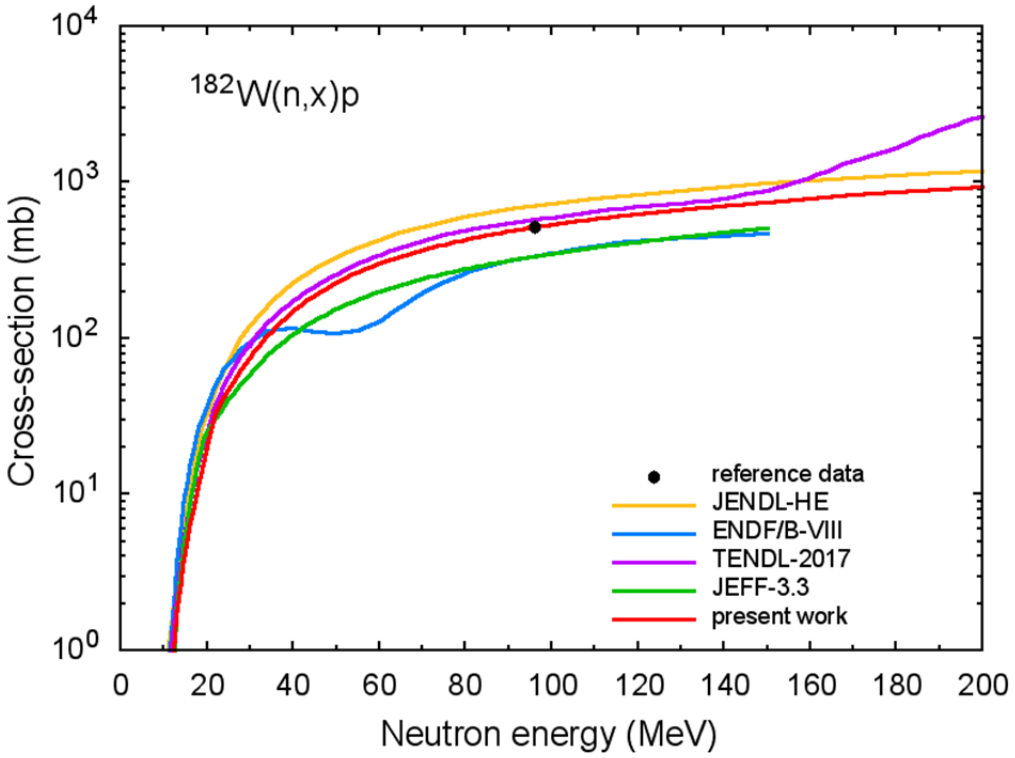

Fig.20 The same as in Fig.19, but on a logarithmic scale.

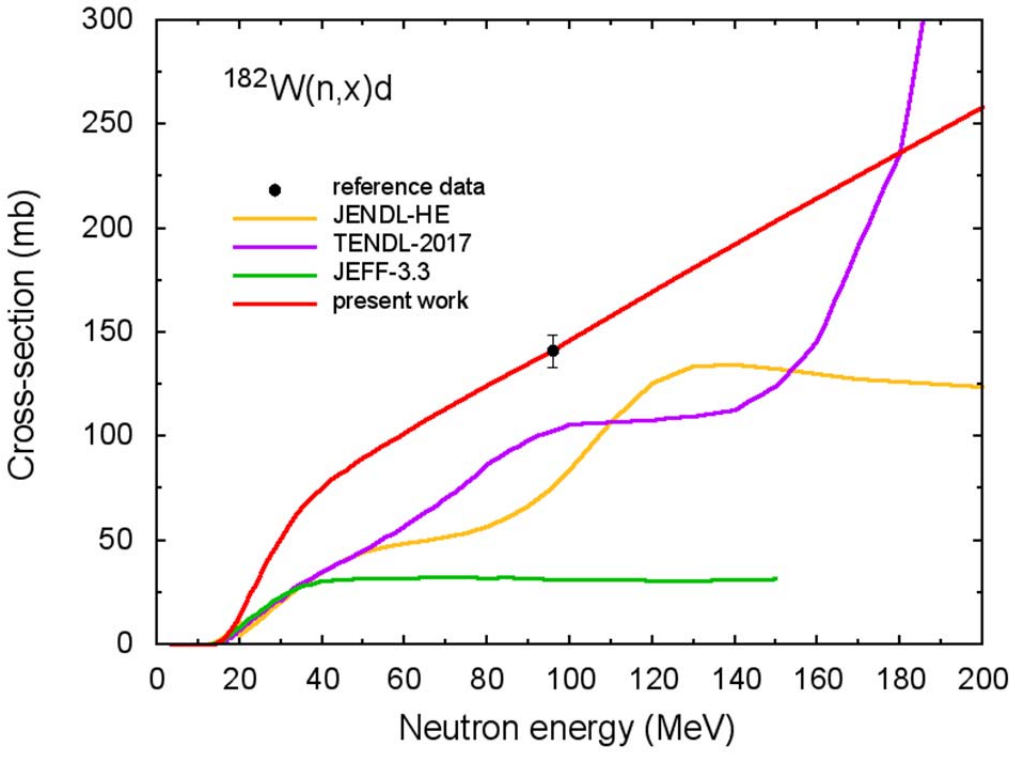

Fig.21 The deuteron production cross-section for ^{182}W.

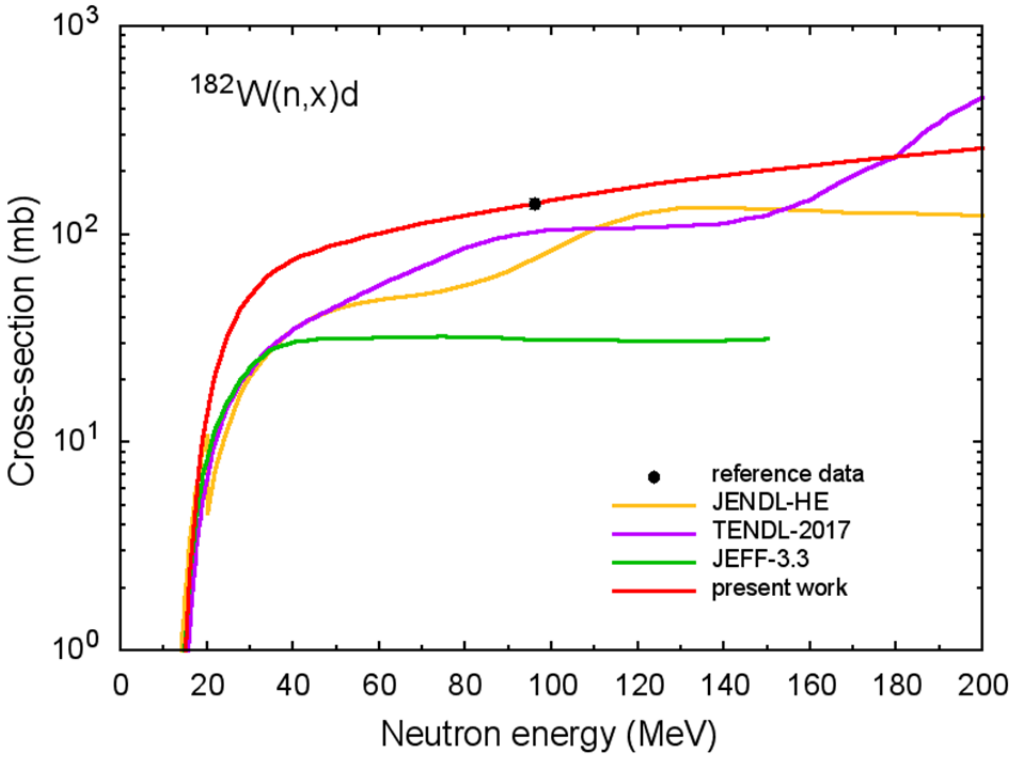

Fig.22 The same as in Fig.21, but on a logarithmic scale.

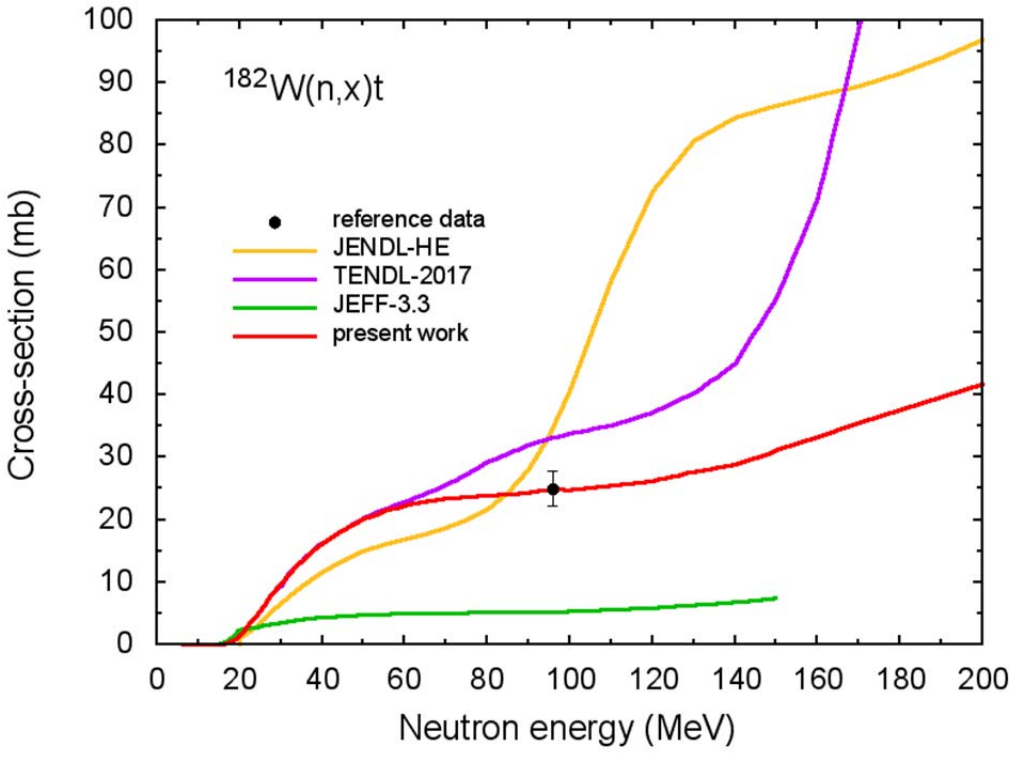

Fig.23 The triton production cross-section for ^{182}W.

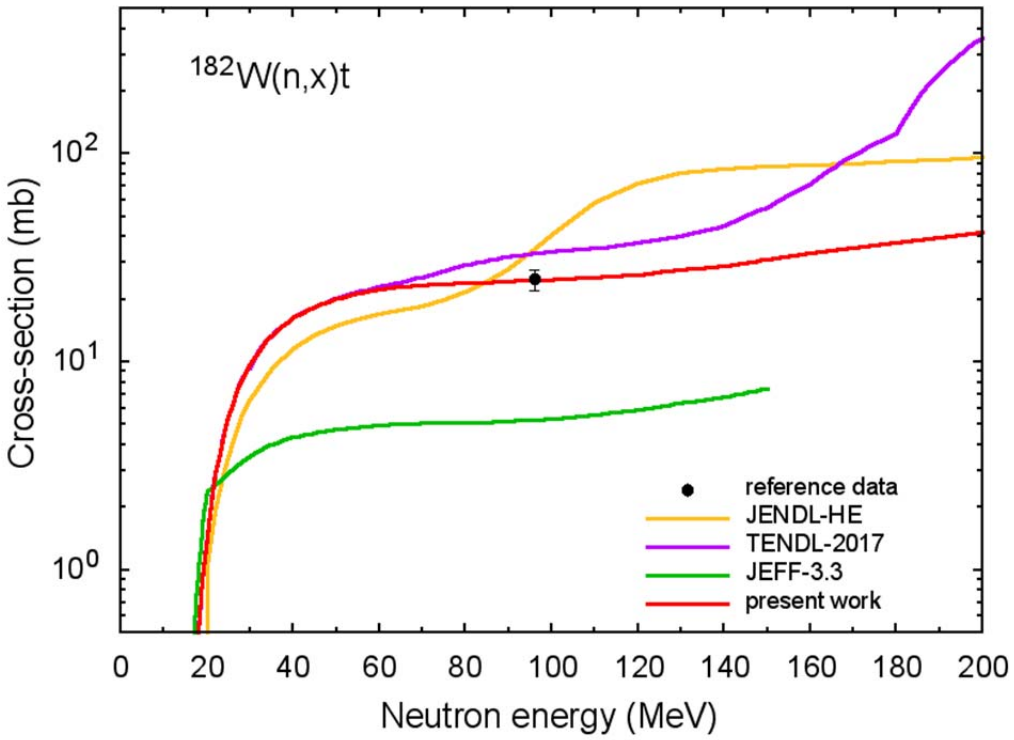

Fig.24 The same as in Fig.23, but on a logarithmic scale.

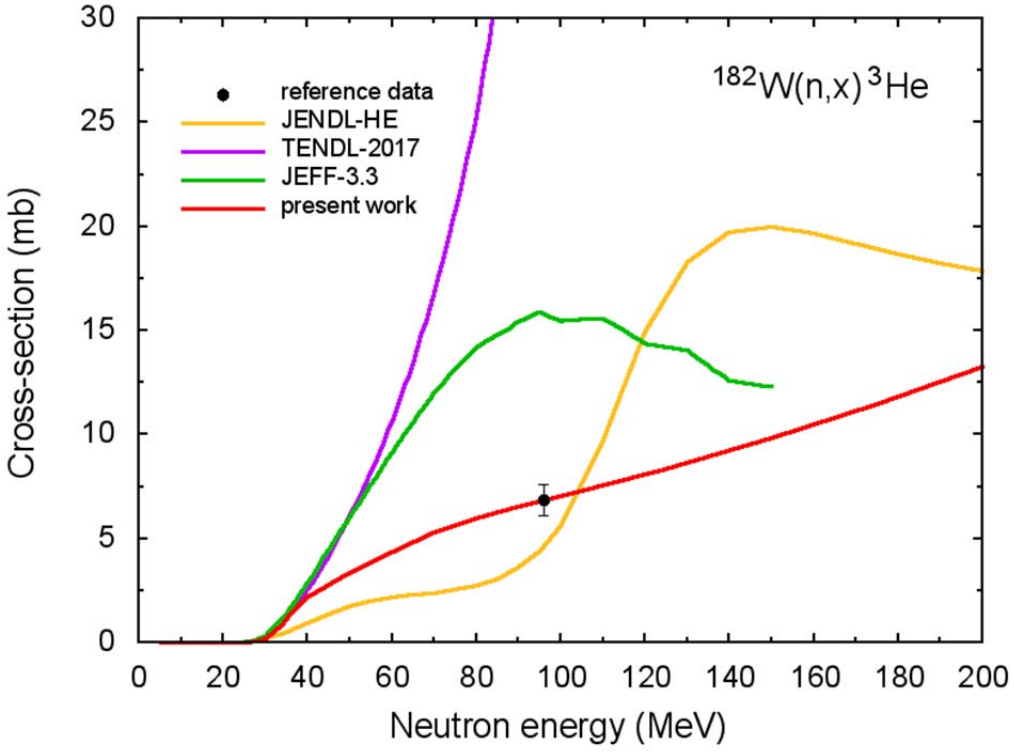

Fig.25 The ^{3}He production cross-section for ^{182}W.

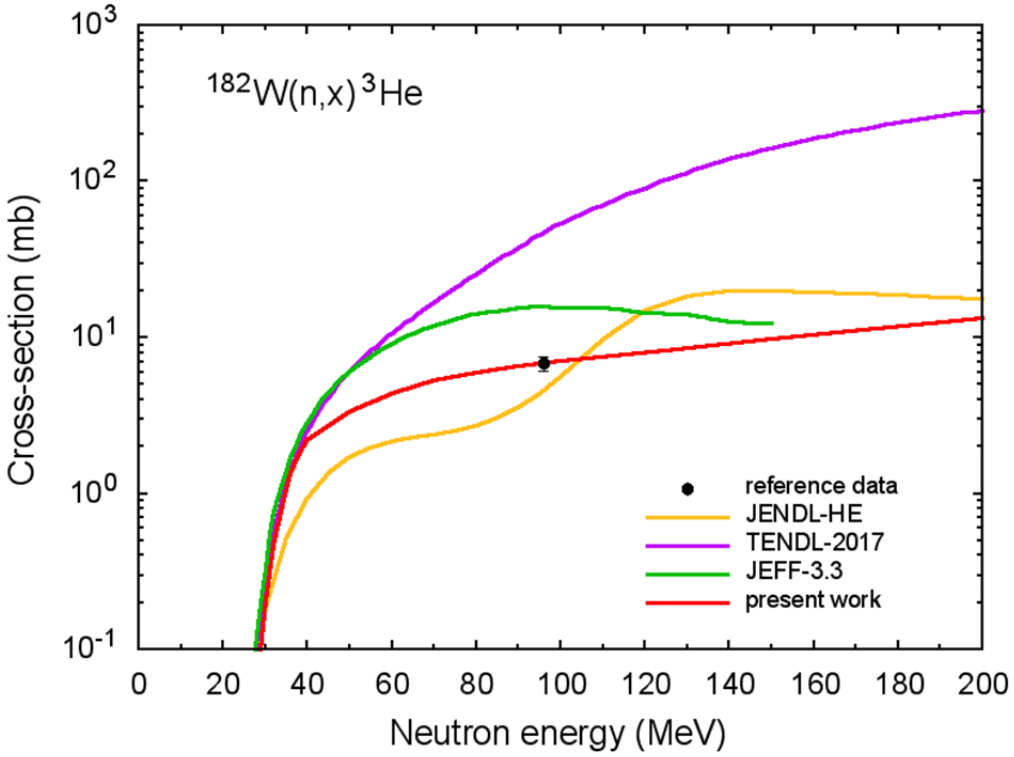

Fig.26 The same as in Fig.25, but on a logarithmic scale.

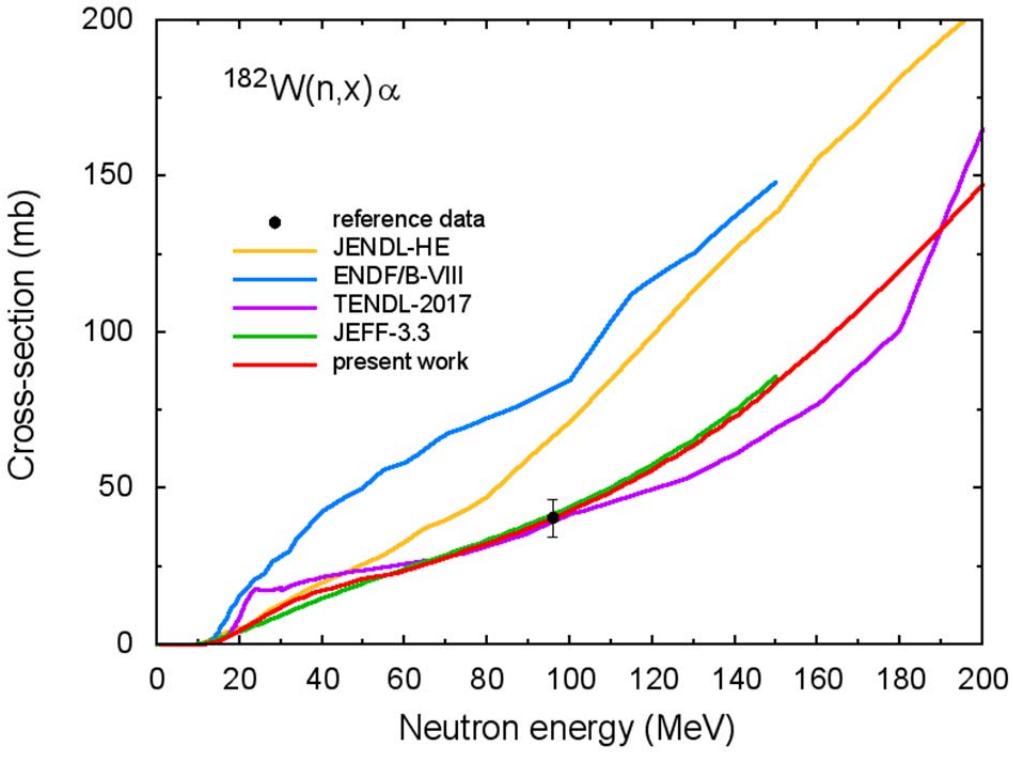

Fig.27 The α-particle production cross-section for ^{182}W.

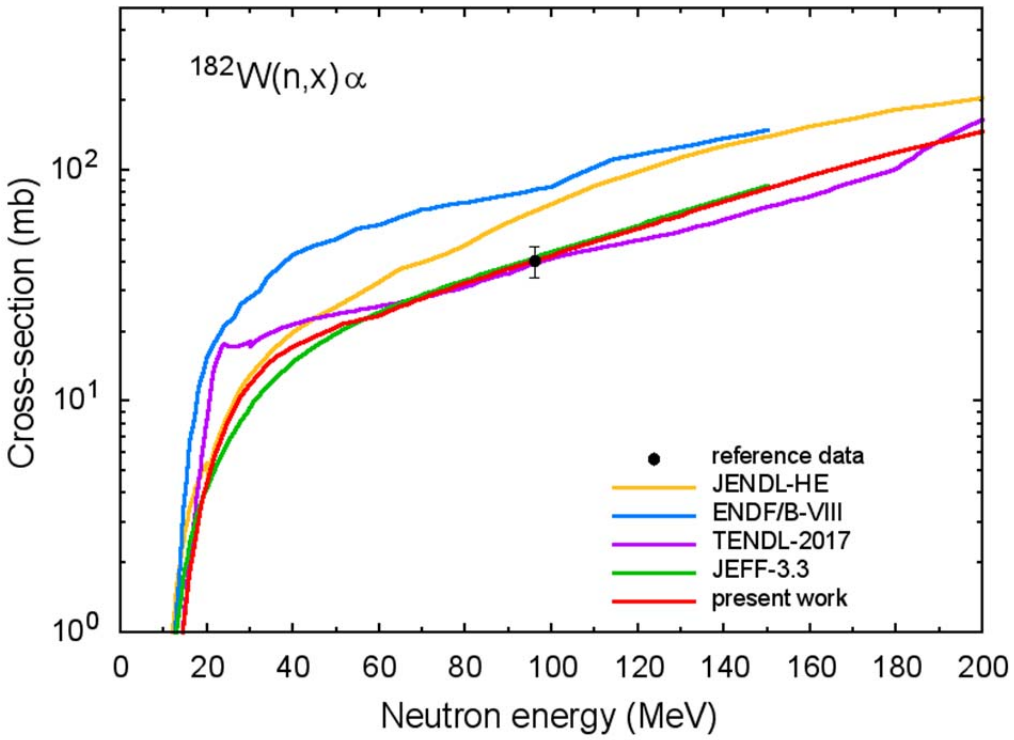

Fig.28 The same as in Fig.27, but on a logarithmic scale.

3.6 Atomic displacement cross-section

Figure 29 shows atomic displacement cross-section (σ_d) for ^{182}W calculated using obtained data and data from different libraries with the NJOY code. The average threshold displacement energy is taken equal to 90 eV. Fig.29 shows also the σ_d values calculated using the CEM03 code with the added elastic components of displacement cross-sections obtained in the present work. At primary neutron energies above 50 MeV the contribution of elastic scattering to the total displacement cross section is less than 10 percent. Obtained data are consistent with calculations using the cascade exciton evaporation model from CEM03, justified at intermediate and high energies.

3.7 Covariance matrices

Figure 30 shows examples of covariance matrices for the total and (n,2n) cross-sections obtained using results of model calculations and experimental data. Calculations were performed using BEKED.

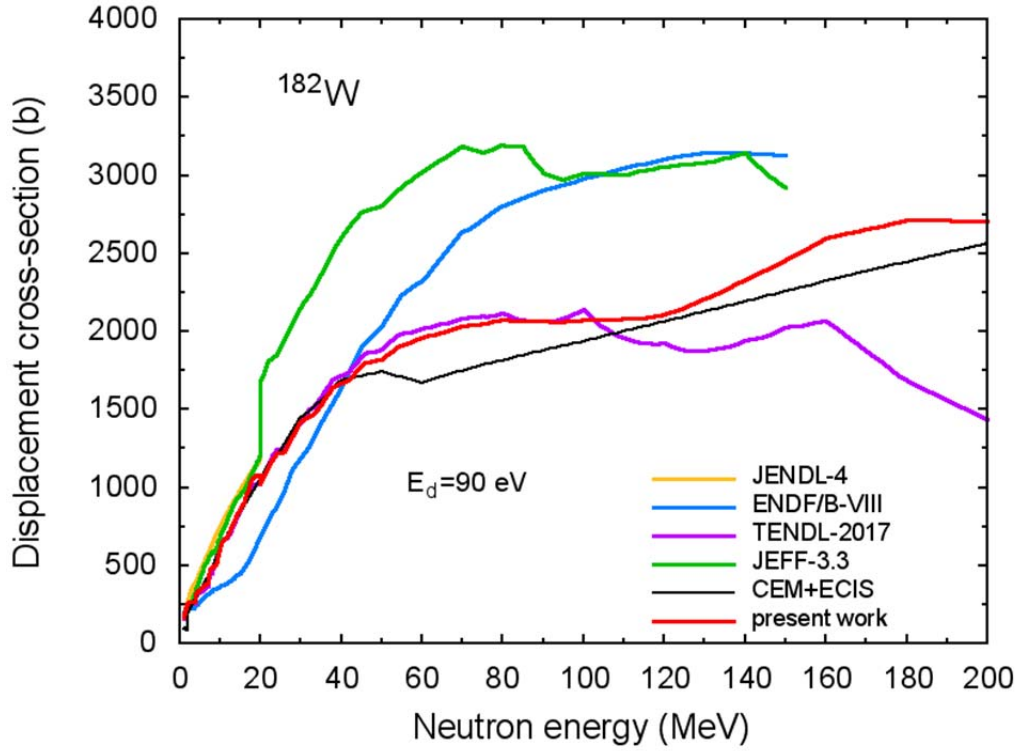

Fig.29 The atomic displacement cross-section for ^{182}W.

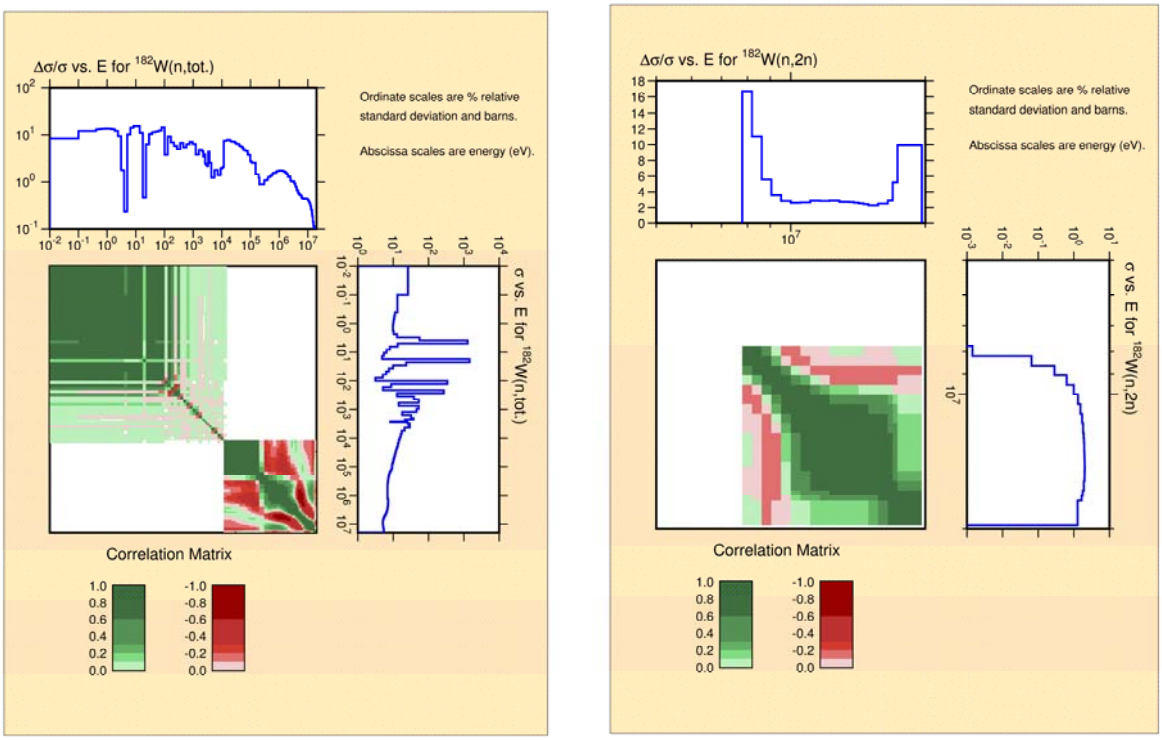

Fig.30 Example of covariance matrices calculated for total cross-section and (n,2n) cross-section for ^{182}W. Plots were prepared using the NJOY code.

4. DATA OBTAINED FOR ^{186}W

4.1 Total and elastic cross-section

Figures 31 and 32 show evaluated total and elastic cross-sections, data from different libraries, and experimental data.

Obtained total cross-sections are in general agreement with experimental data and are close to JENDL-4/HE cross-sections at neutron energies below 1 MeV. All evaluated data agree with the measurements [25] at energies above 15 MeV.

Elastic cross-section obtained in the present work are close to evaluated cross-sections from libraries and available experimental data (Fig.32).

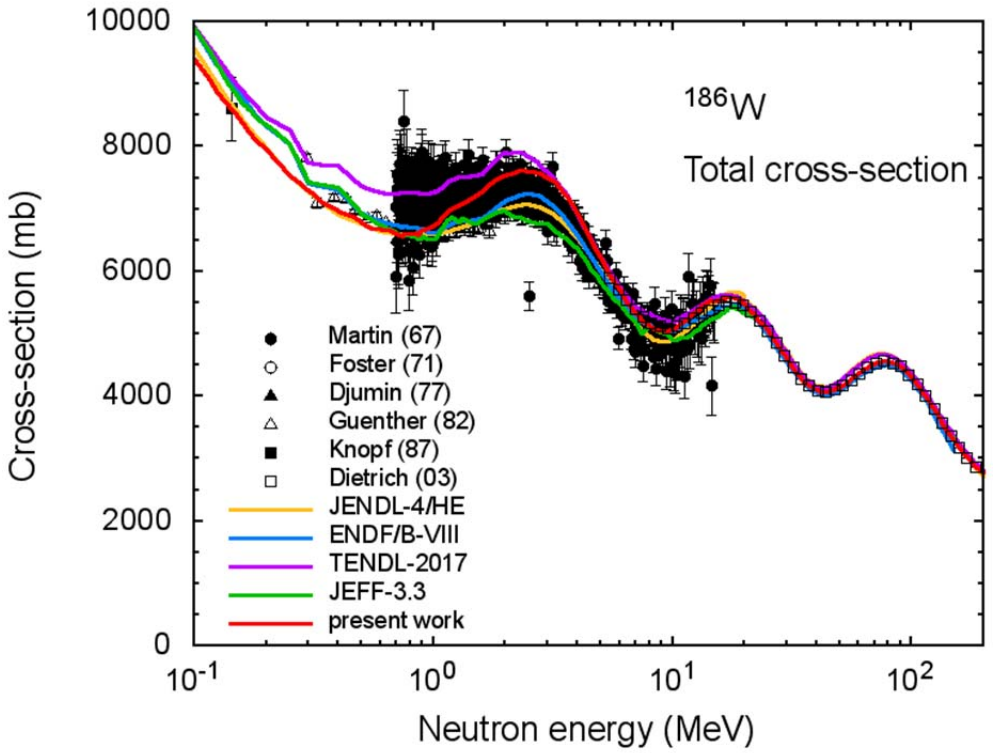

Fig.31 The total reaction cross-section for neutron irradiation of ^{186}W evaluated in the present work, measured data, and data taken from different libraries.

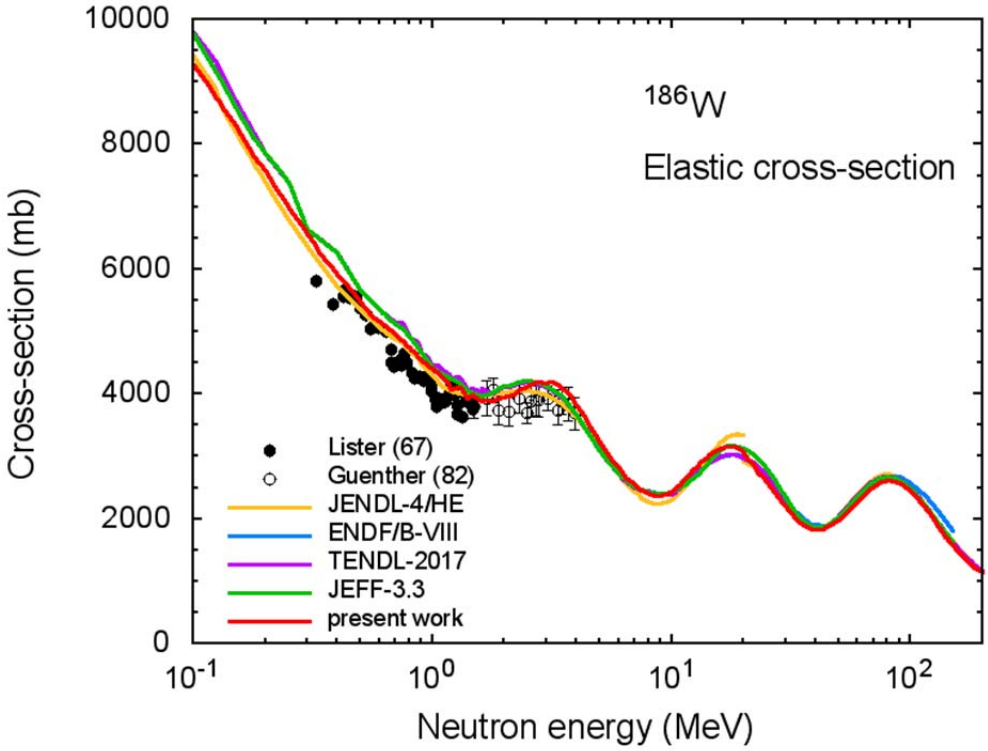

Fig.32 The elastic cross-section ^{186}W evaluated in the present work, measured data, and data taken from different libraries.

4.2 Inelastic scattering

Inelastic neutron scattering cross-sections with excitation of different levels of ^{186}W are shown in Figs.33-36. The data are recorded in the ENDF file in sections with MT numbers 51-53 and 57.

Evaluated cross-sections agree with available experimental data [34,52].

4.3 Various reactions

Figures 37-46 show evaluated cross sections for different reactions on ^{186}W. For a better illustration, the (n,p) and (n,α) reaction cross sections are shown on linear scale (Figs.43,45) and logarithmic scale (Figs.44,46).

In general, data obtained are in good agreement with measured data.

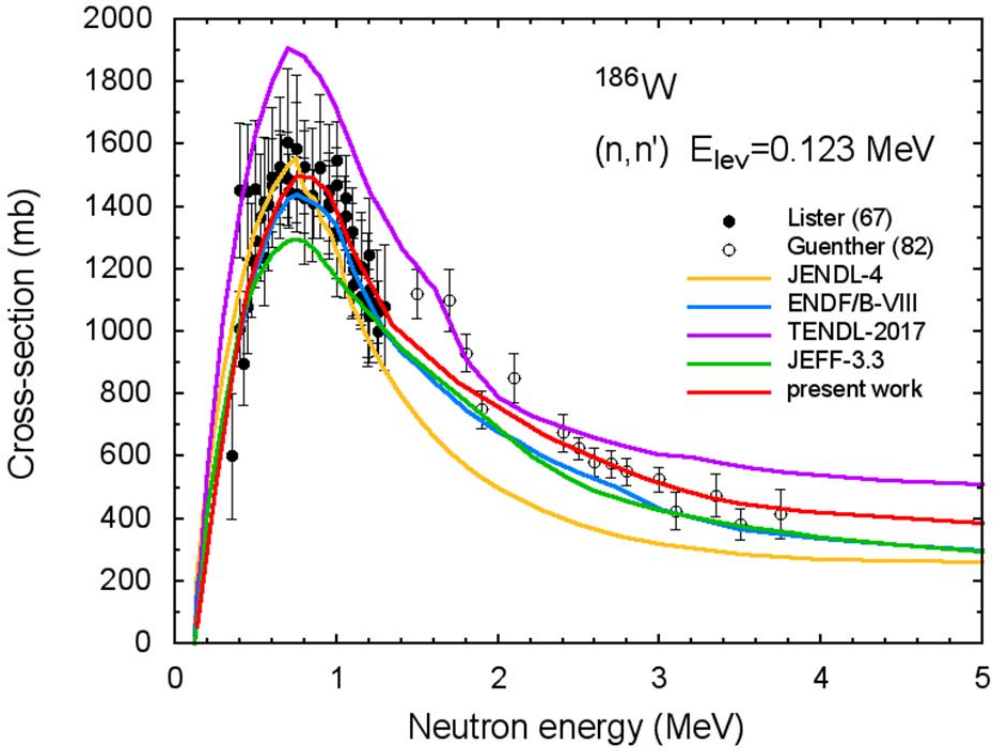

Fig.33 The inelastic scattering cross-section ^{186}W(n,n') with excitation of the level 0.12263 MeV (2^+).

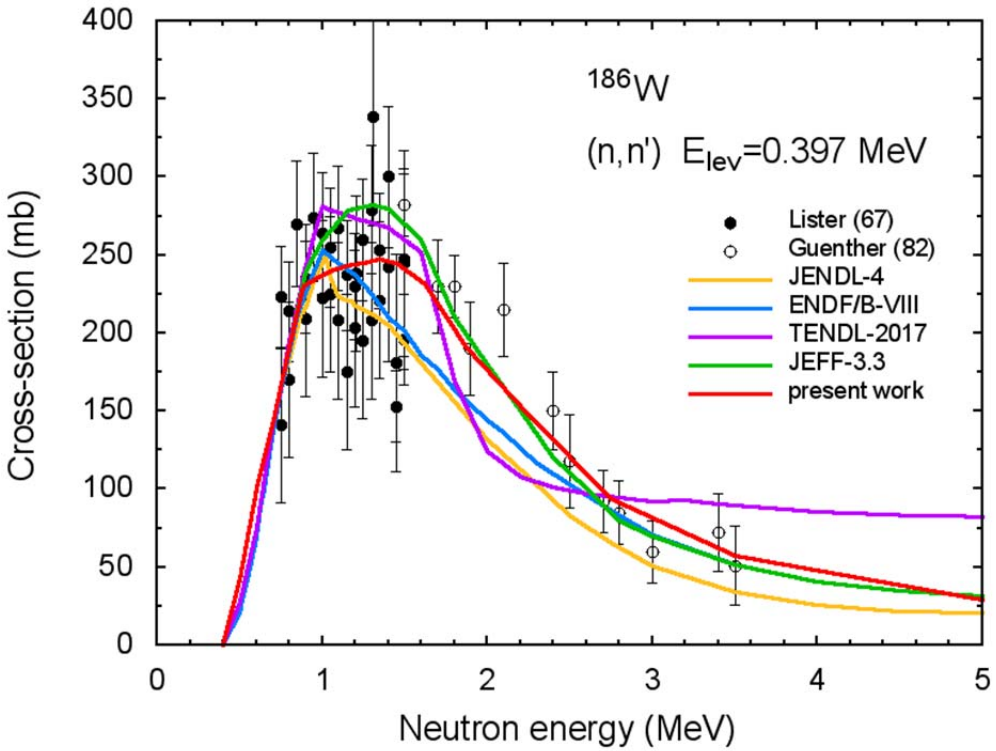

Fig.34 The inelastic scattering cross-section ^{186}W(n,n') with excitation of the level 0.39655 MeV (4^+).

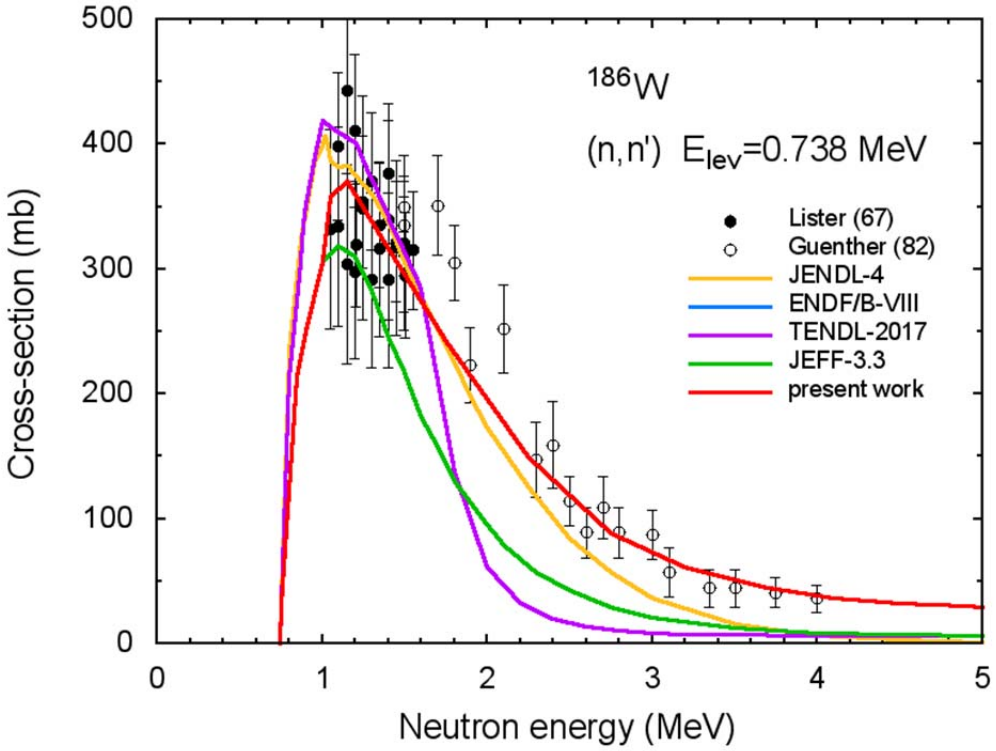

Fig.35 The inelastic scattering cross-section ^{186}W(n,n') with excitation of the level 0.73796 MeV (2^+).

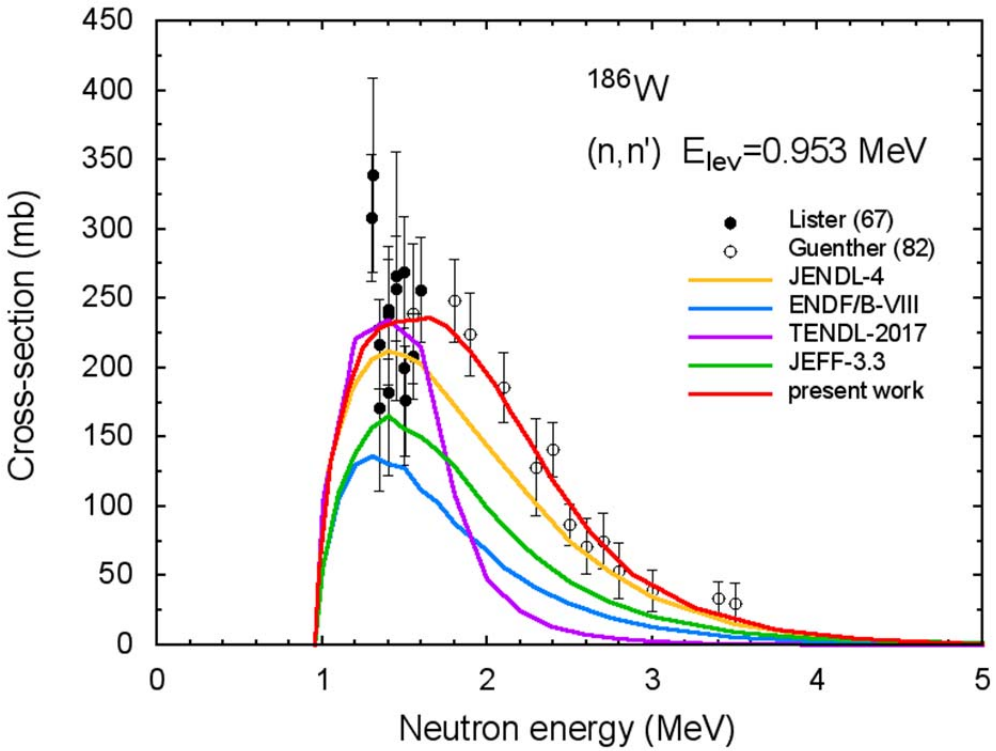

Fig.36 The inelastic scattering cross-section ^{186}W(n,n') with excitation of the level 0.95274 MeV (2^-).

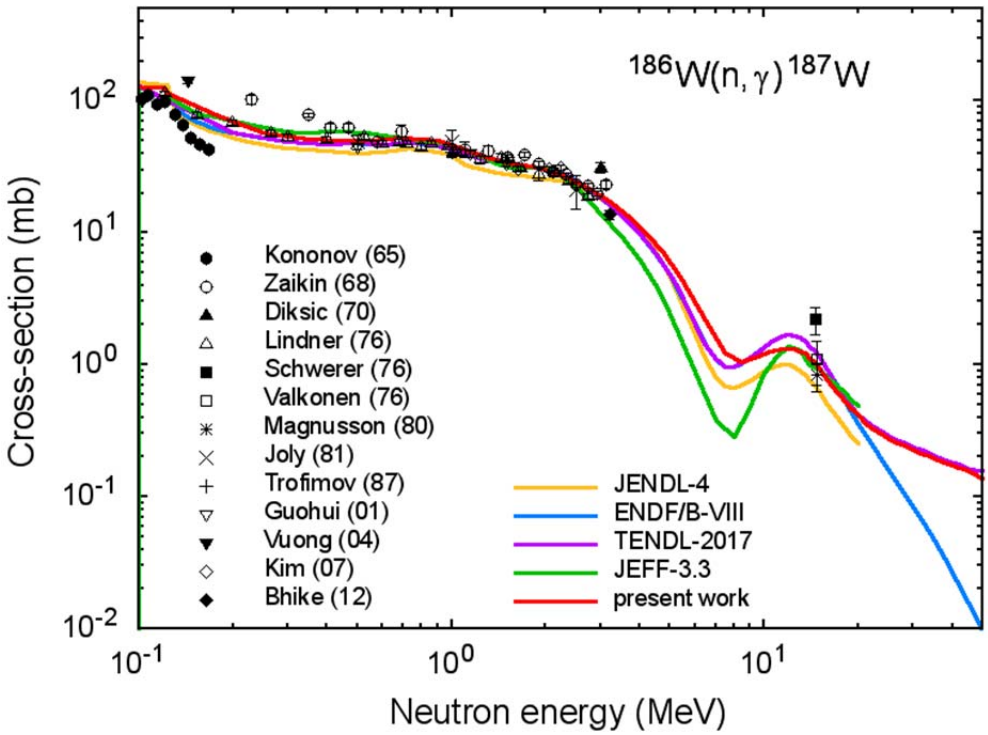

Fig.37 The (n,γ) reaction cross-section for ^{186}W.

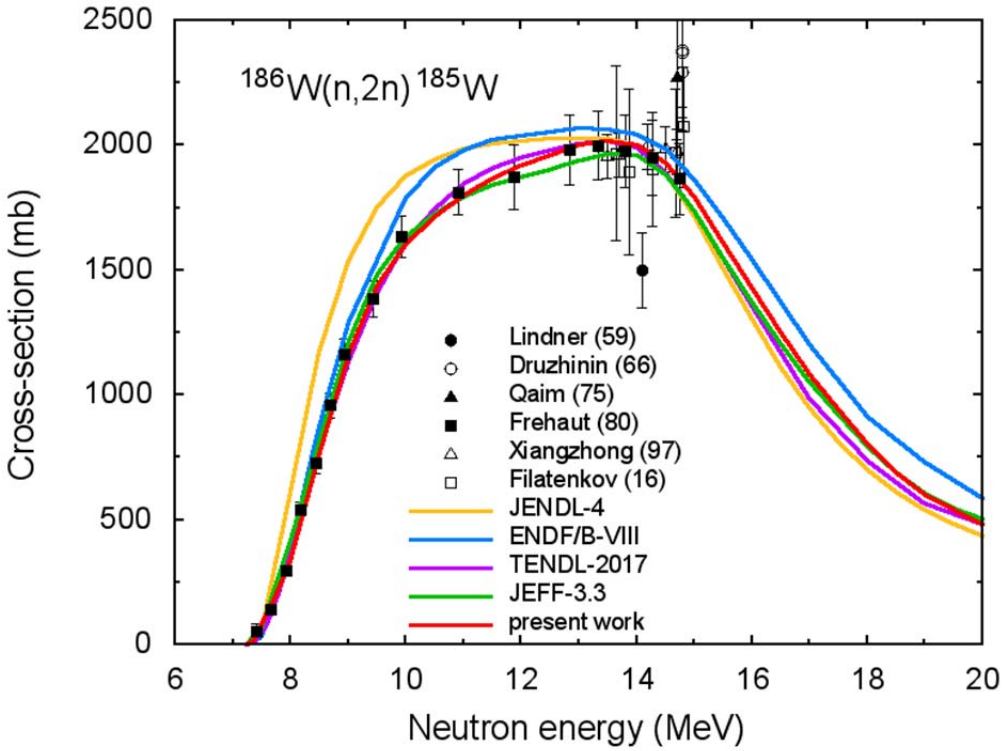

Fig.38 The (n,2n) reaction cross-section for ^{186}W.

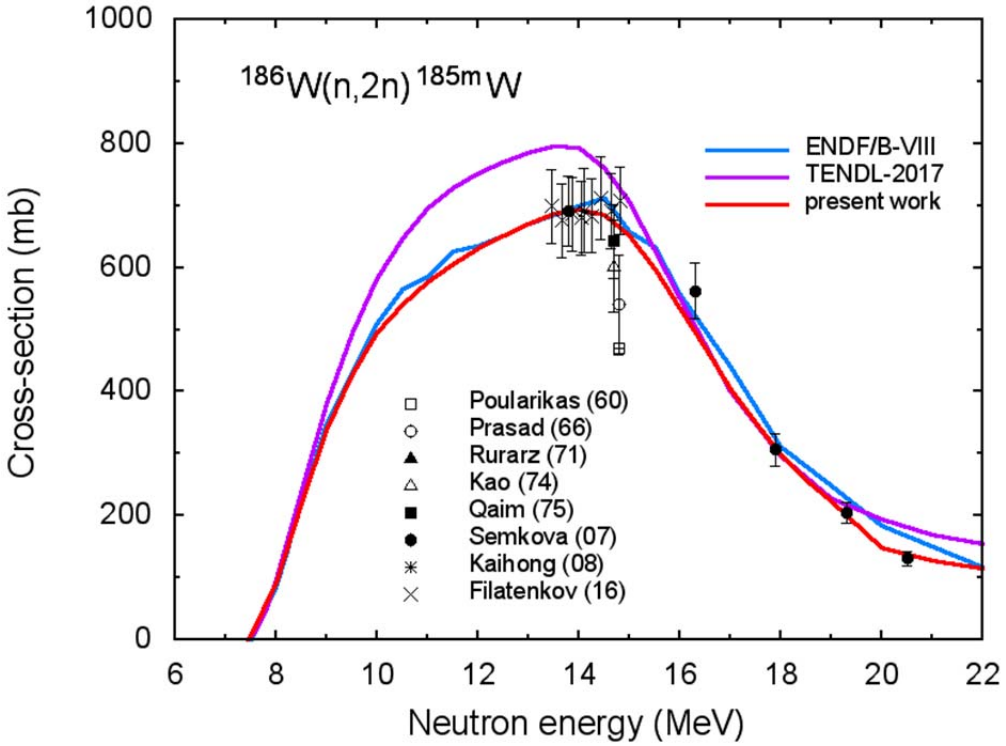

Fig.39 The ^{186}W(n,2n)^{185m}W reaction cross-section.

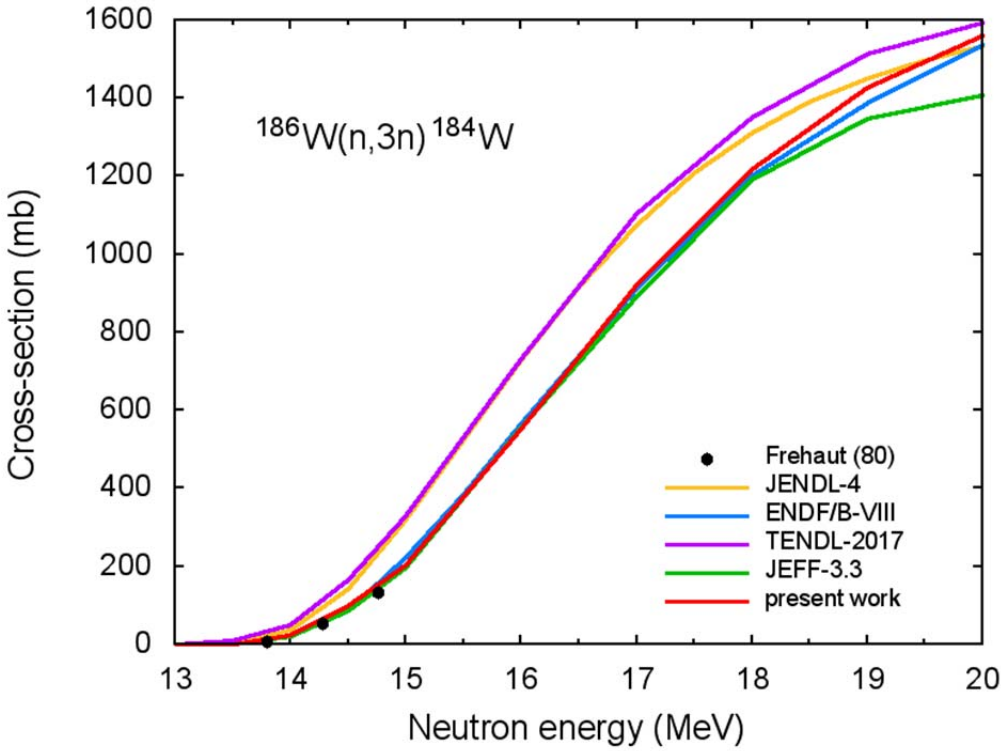

Fig.40 The (n,3n) reaction cross-section for ^{186}W.

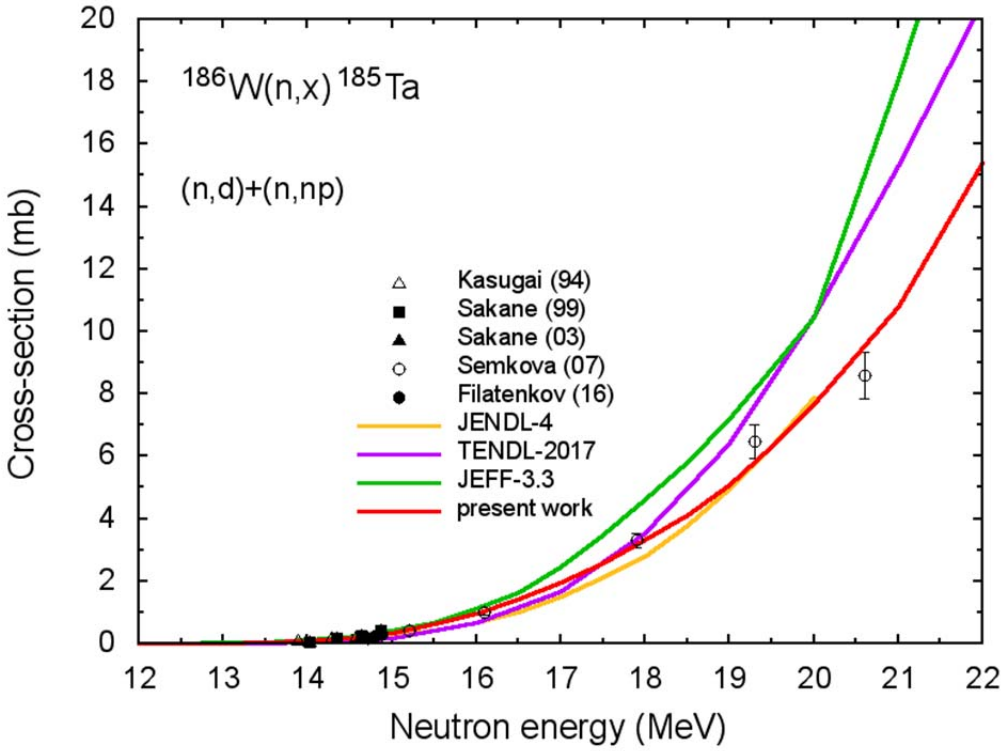

Fig.41 The sum of (n,d) and (n,np) reaction cross-sections for ^{186}W.

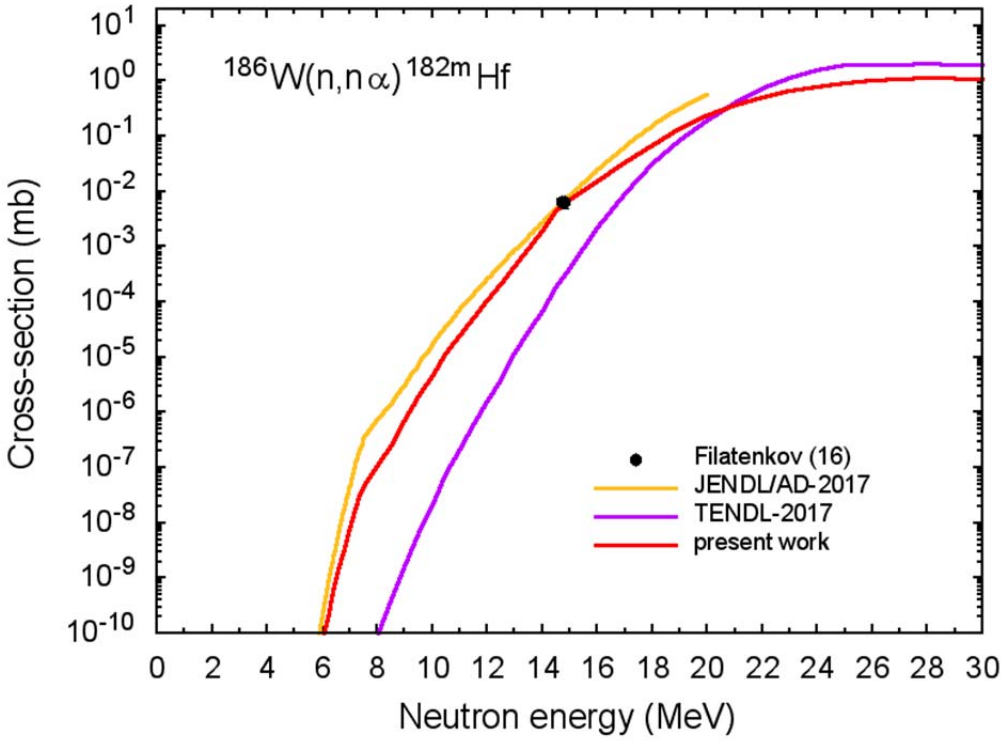

Fig.42 The ^{186}W(n,nα)^{182m}Hf reaction cross-section.

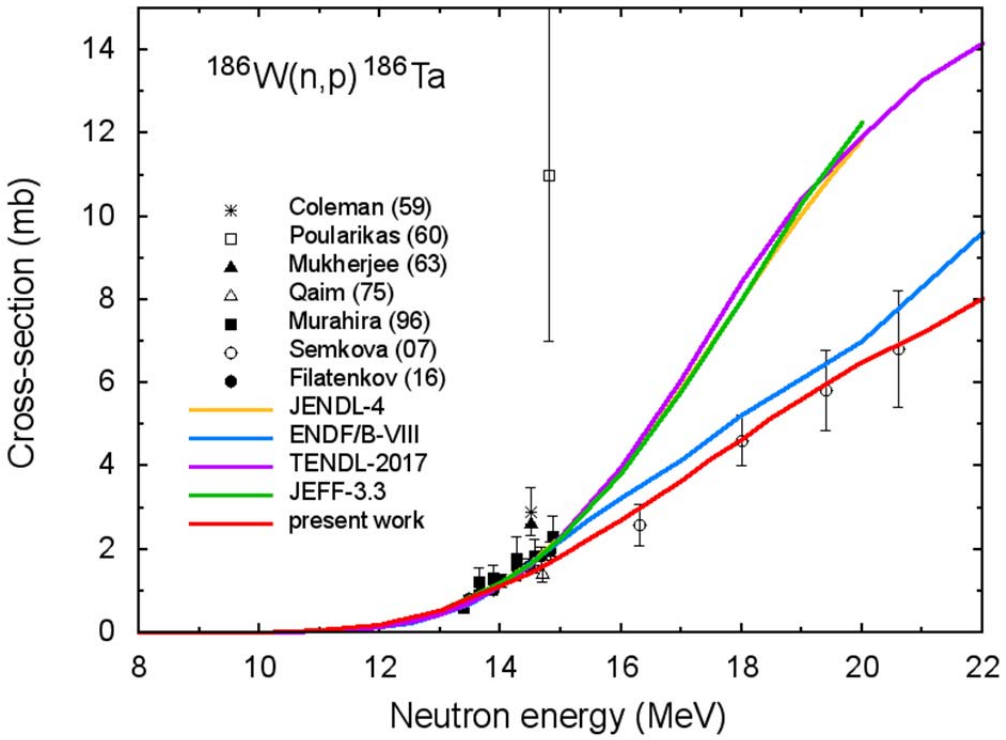

Fig.43 The (n,p) reaction cross-section for ^{186}W.

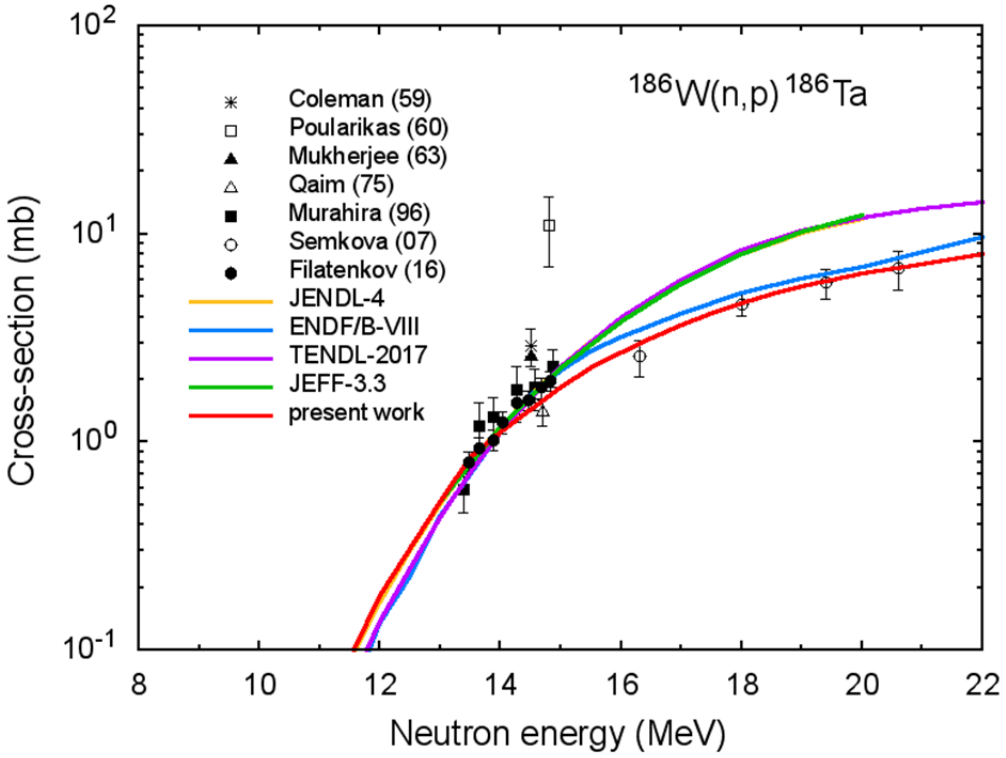

Fig.44 The same as in Fig.43, but on a logarithmic scale.

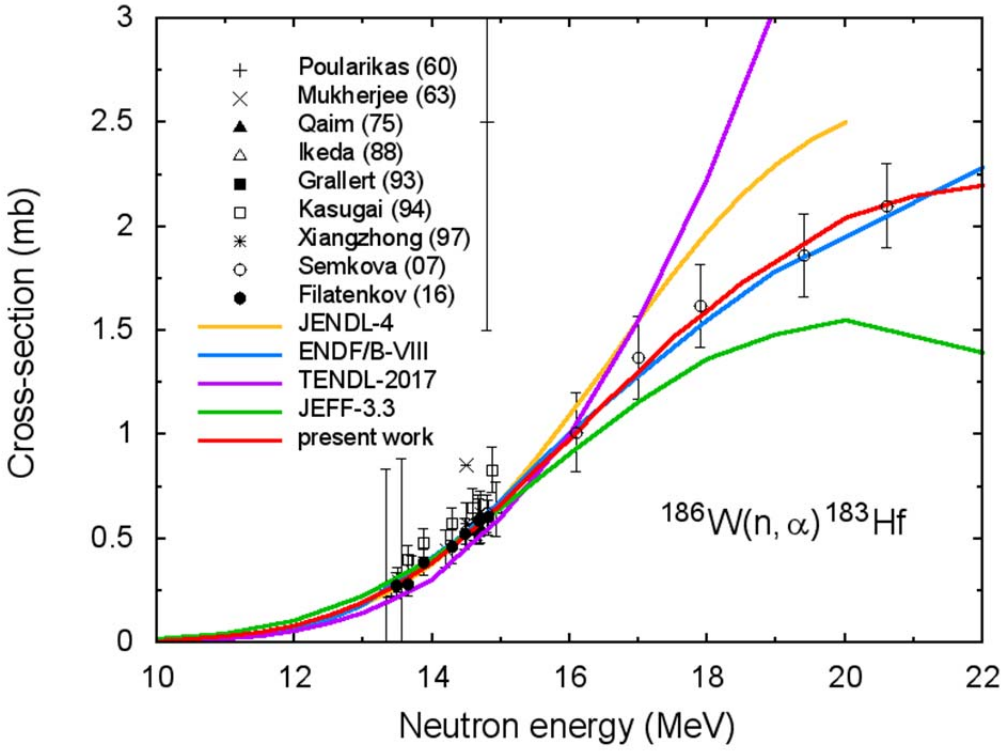

Fig.45 The (n,α) reaction cross-section for ^{186}W.

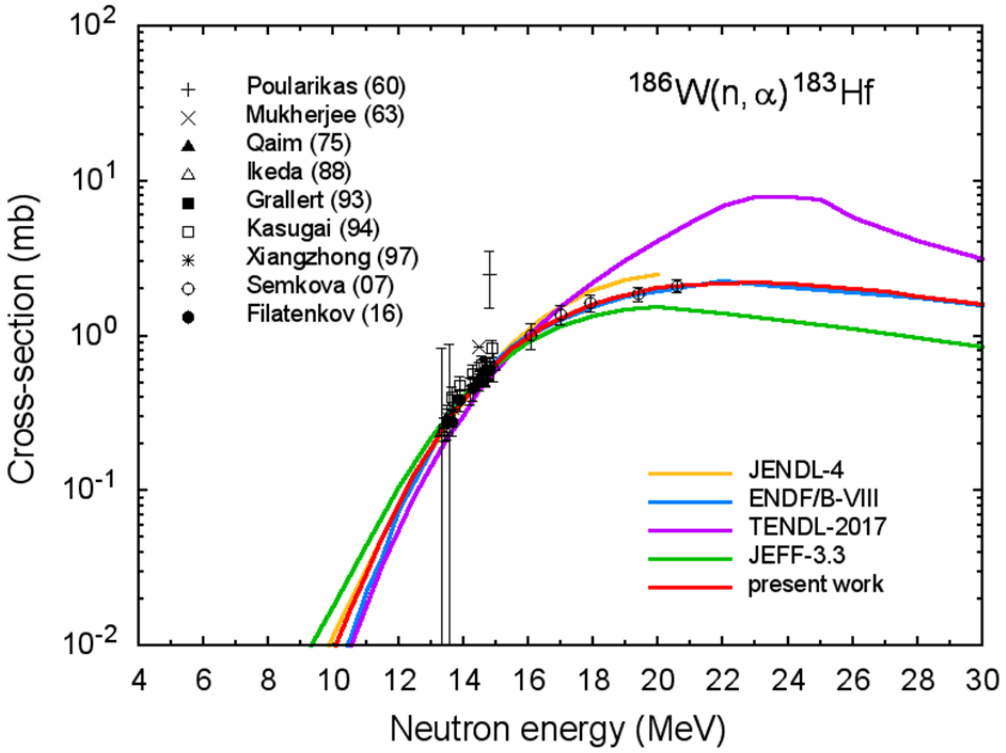

Fig.46 The same as in Fig.45, but on a logarithmic scale.

4.4 Neutron energy distribution

As for ^{182}W, measurements of neutron spectra for ^{186}W are absent. Fig.47 shows the measured data for the natural mixture of tungsten isotopes and the evaluated data for ^{186}W for neutron incident energy 14.1 MeV. The comparison is only a very approximate test of the spectrum obtained.

Figure 48 shows the neutron energy distribution obtained in the present work and taken from different data libraries. There is a smaller scatter of evaluated data than for ^{182}W (Fig.17).

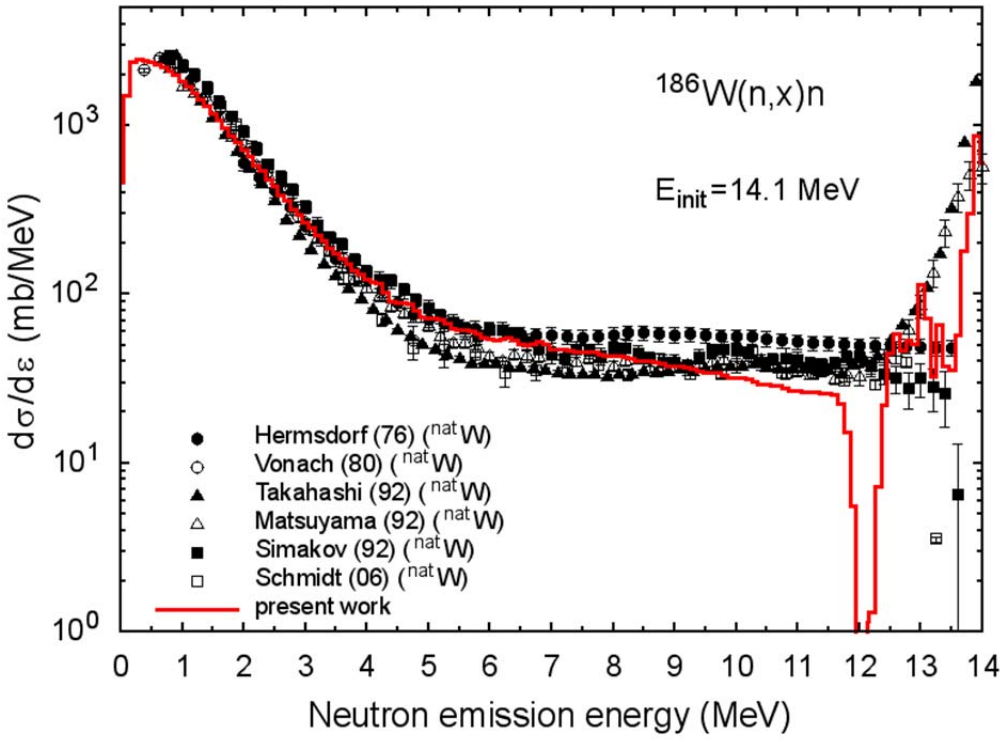

Fig.47 The neutron energy distributions in ^{186}W(n,x)n reaction induced by 14.1 neutrons obtained in the present work and measured for natural mixture of tungsten isotopes.

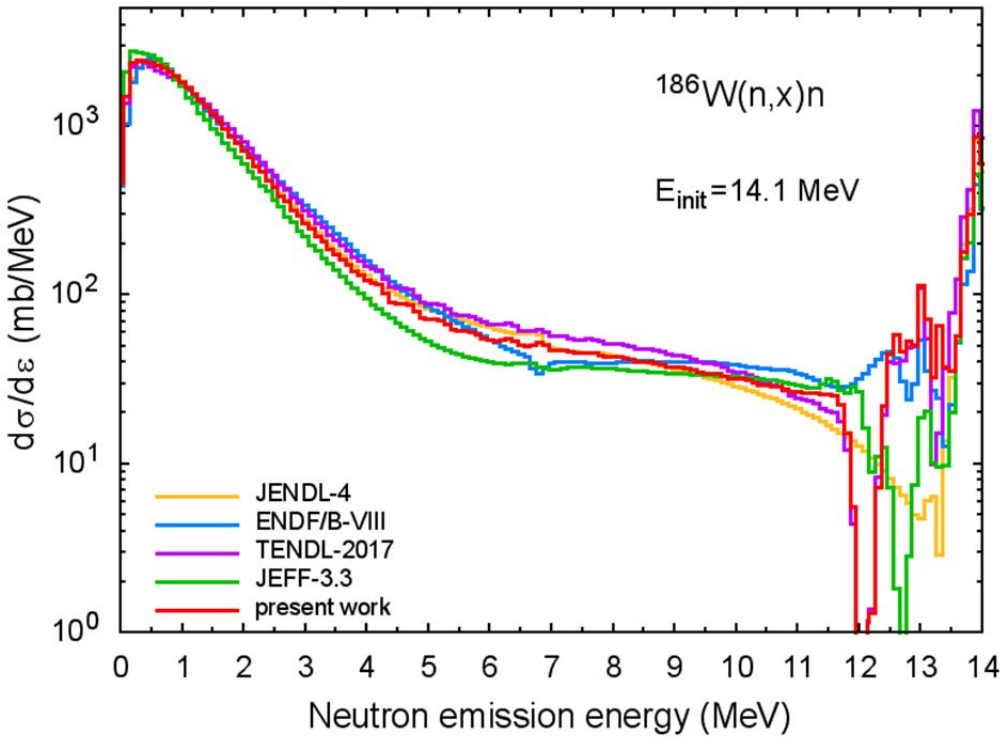

Fig.48 The neutron energy distributions in ^{186}W(n,x)n reaction induced by 14.1 MeV neutrons obtained in the present work and taken from various data libraries.

4.5 Light particle production cross-sections

Figure 49 illustrates the neutron production cross-section, and Figs.50-59 show components of hydrogen and helium production cross sections for n+^{186}W interactions. For comparison, cross-sections calculated using the intranuclear cascade evaporation model [101-104] (Fig.49), "reference" data obtained from the evaluation of A-dependence of cross-sections [105,106] (Figs.50-59), and cross-sections from different data libraries are plotted.

The obtained cross sections are consistent with both the calculations and the "reference" data.

4.6 Atomic displacement cross-section

Figure 60 shows the atomic displacement cross-section for ^{186}W calculated using data obtained in the present work. For comparison cross-sections from different libraries and σ_d values calculated using the CEM03 code with the added elastic component of cross-section are shown. Data were processed using the NJOY code.

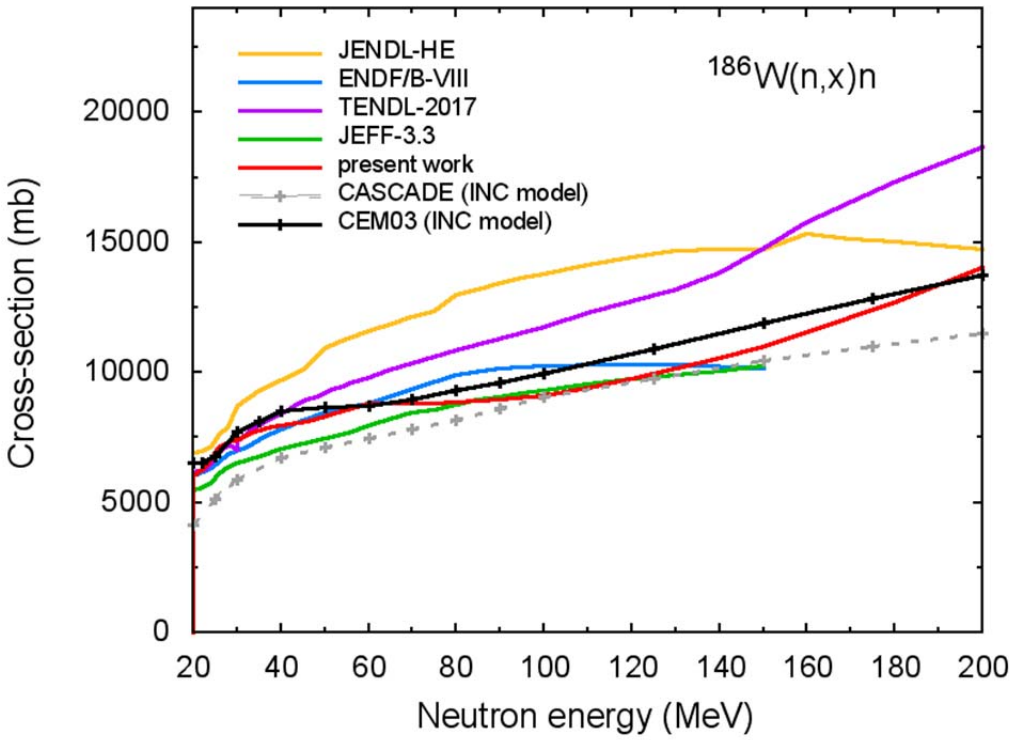

Fig.49 The neutron production cross-section for ^{186}W.

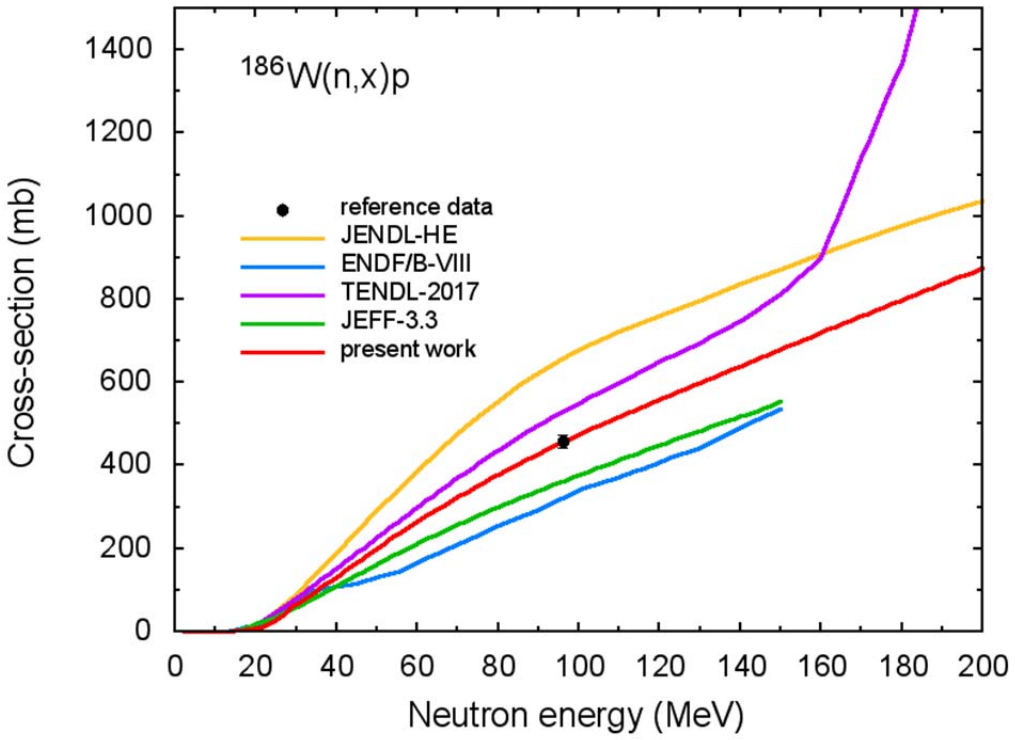

Fig.50 The proton production cross-section for ^{186}W.

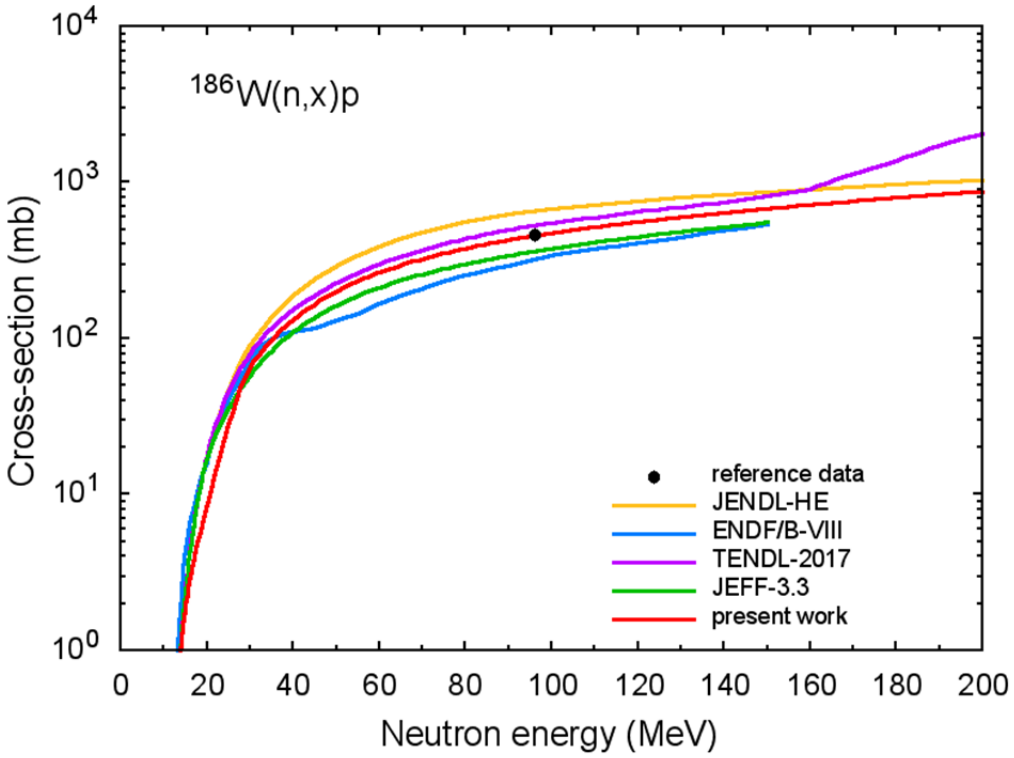

Fig.51 The same as in Fig.50, but on a logarithmic scale.

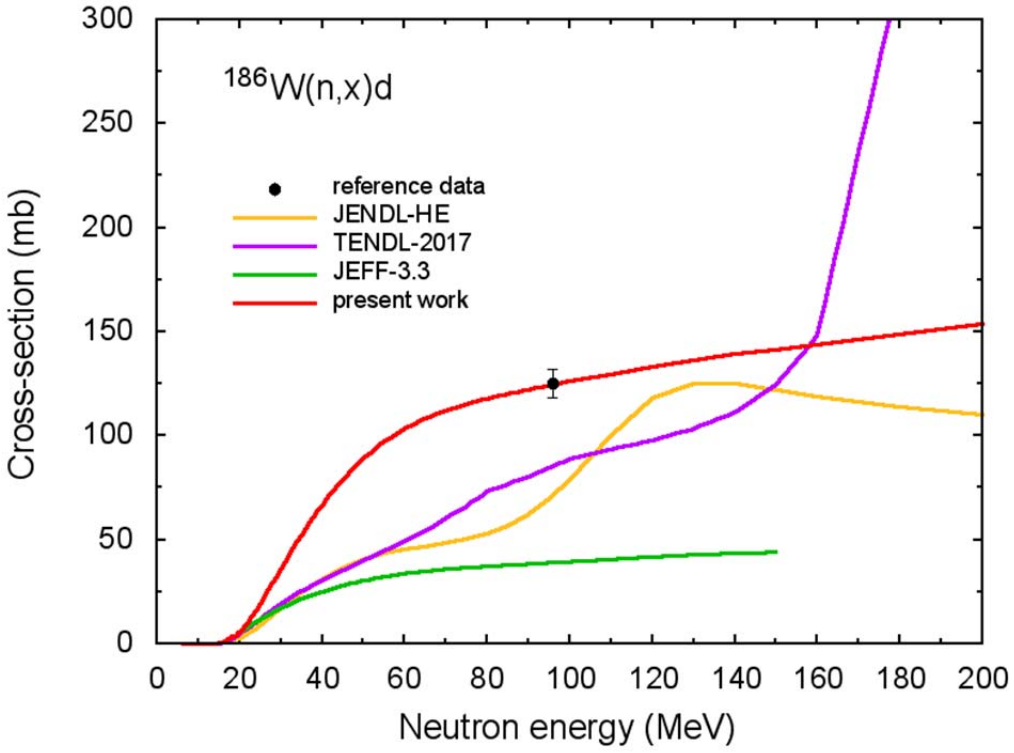

Fig.52 The deuteron production cross-section for ^{186}W.

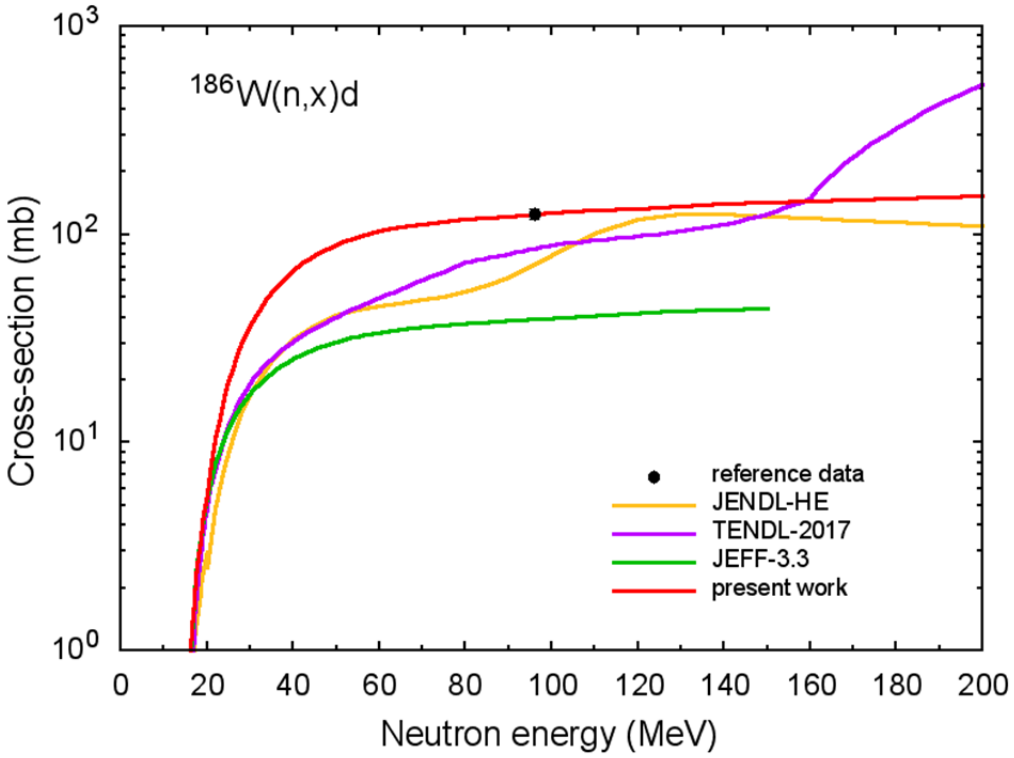

Fig.53 The same as in Fig.52, but on a logarithmic scale.

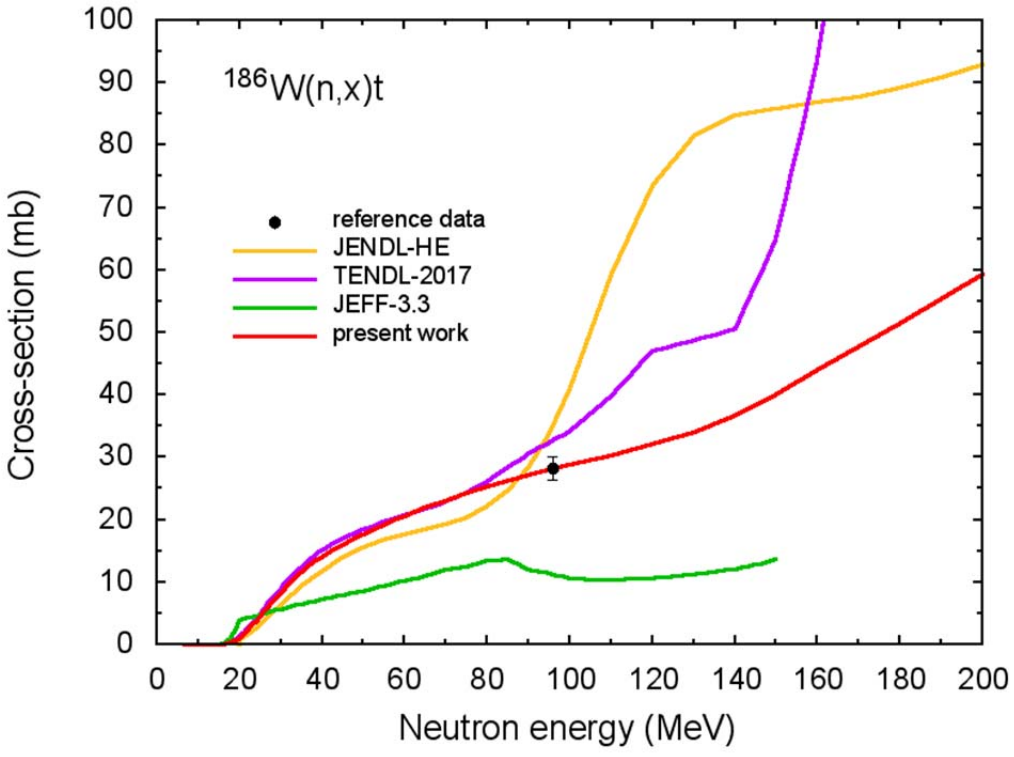

Fig.54 The deuteron production cross-section for ^{186}W.

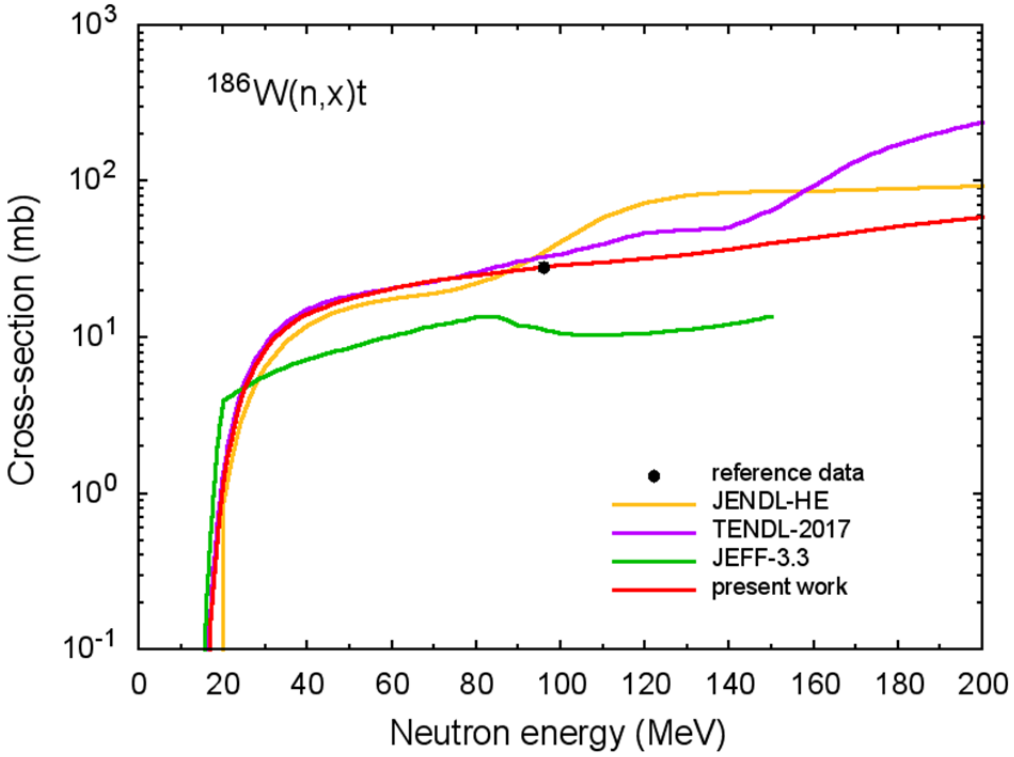

Fig.55 The same as in Fig.54, but on a logarithmic scale.

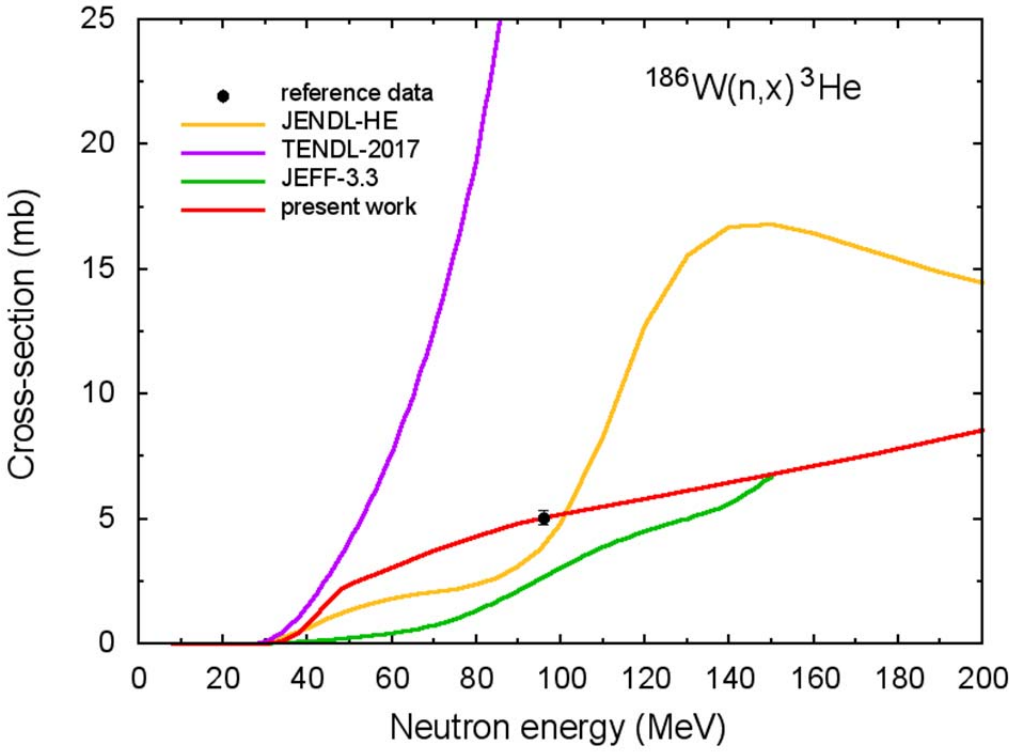

Fig.56 The ^{3}He production cross-section for ^{186}W.

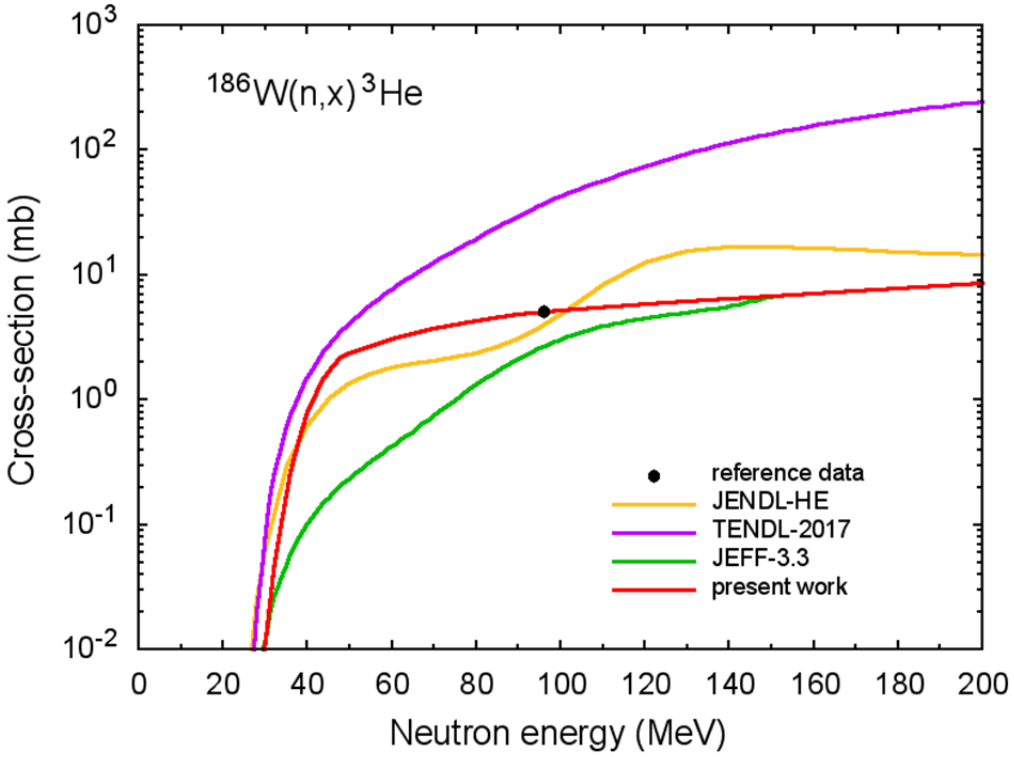

Fig.57 The same as in Fig.56, but on a logarithmic scale.

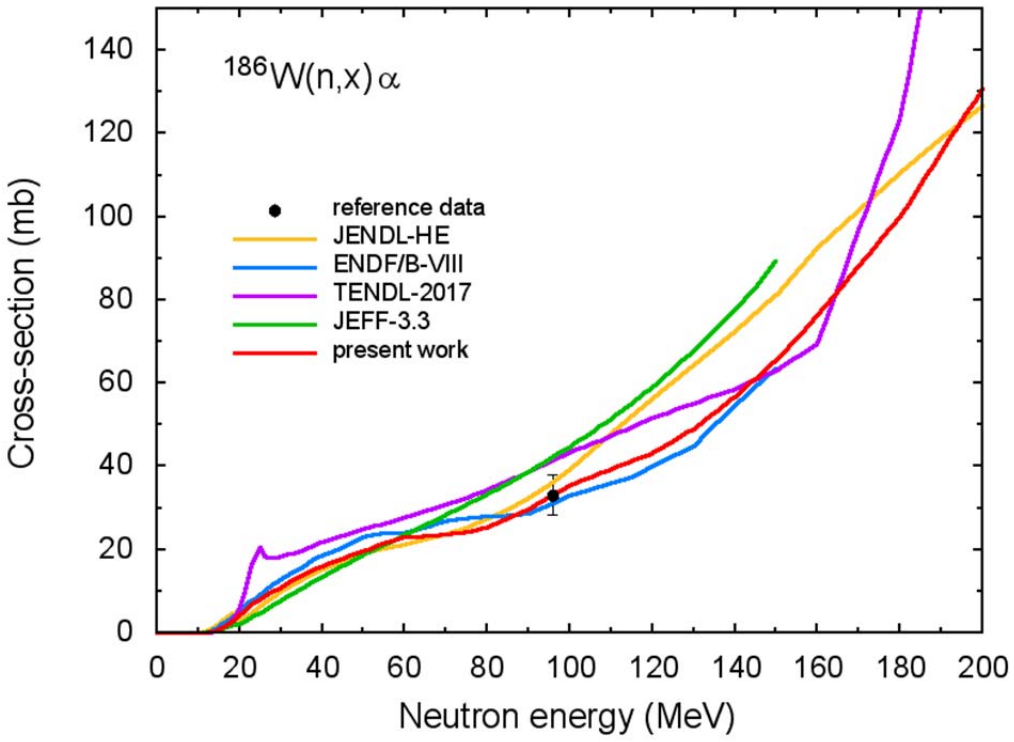

Fig.58 The α-particle production cross-section for ^{186}W.

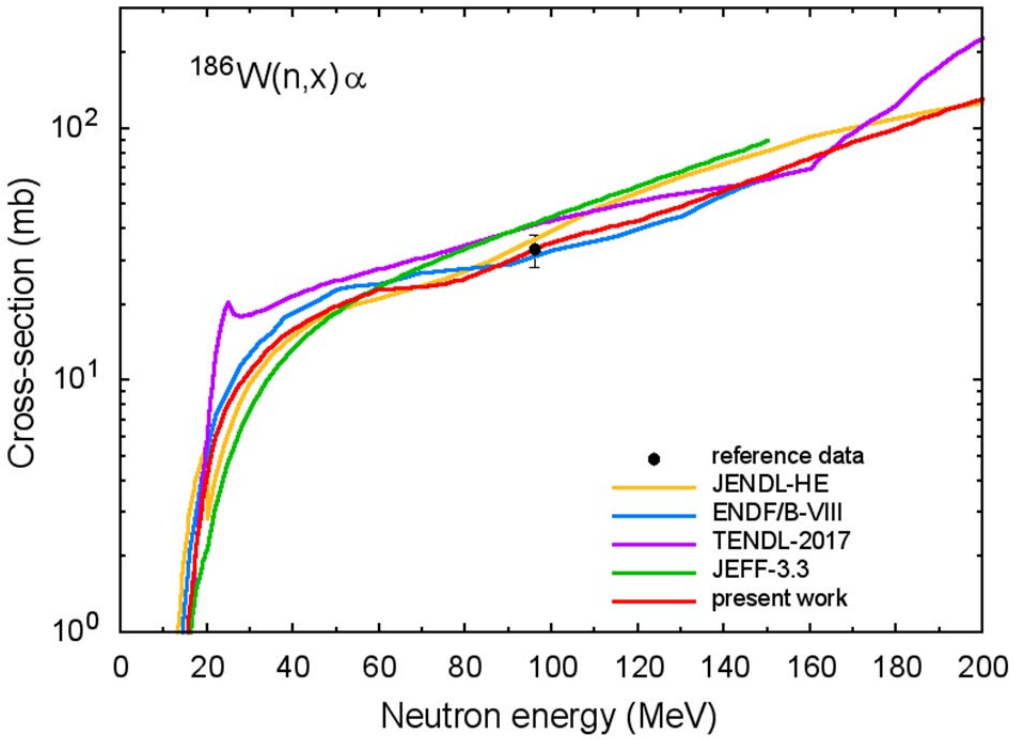

Fig.59 The same as in Fig.58, but on a logarithmic scale.

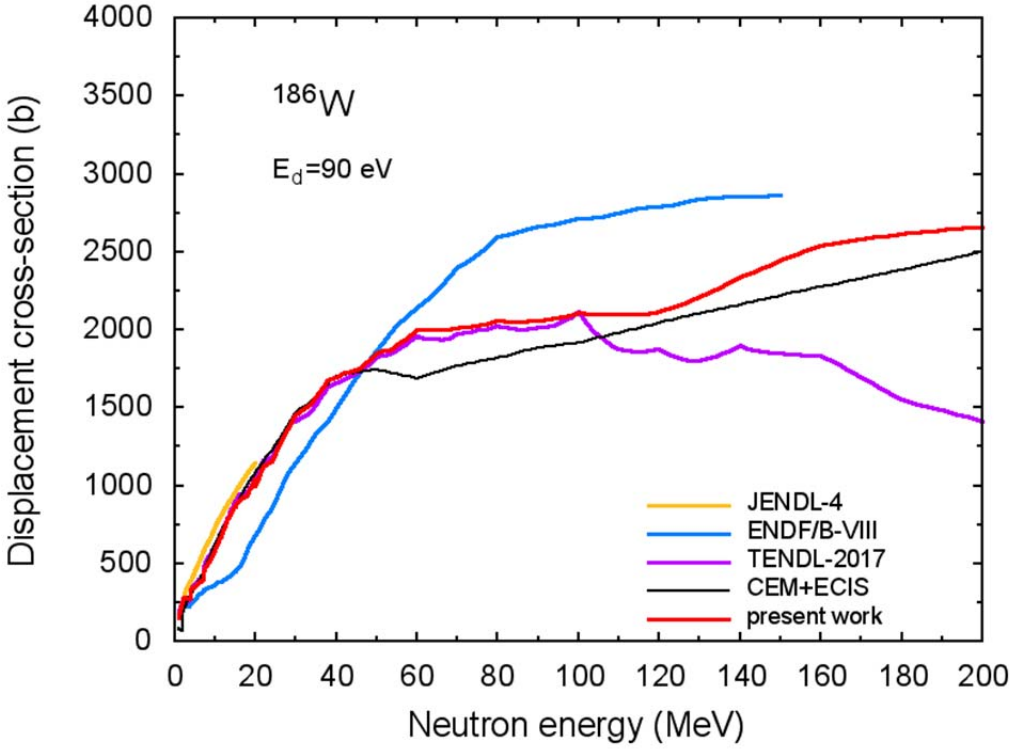

Fig.60 The atomic displacement cross-section for ^{186}W.

4.7 Covariance matrices

Figure 61 shows examples of covariance matrices for the elastic and (n,3n) cross-sections calculated using the results of model calculations and experimental data.

5. CONCLUSION

New general purpose data files were prepared for tungsten isotopes ^{182}W and ^{186}W at primary neutron energy up to 200 MeV. A special version of the TALYS code implementing the geometry dependent hybrid model was applied for calculations of nuclide production and particle energy distributions.

The evaluation of cross-sections was performed using available experimental data, systematics including estimated A-dependence of components of gas production cross-sections, and obtained covariance information. Resonance parametrs were taken from JEFF-3.3.

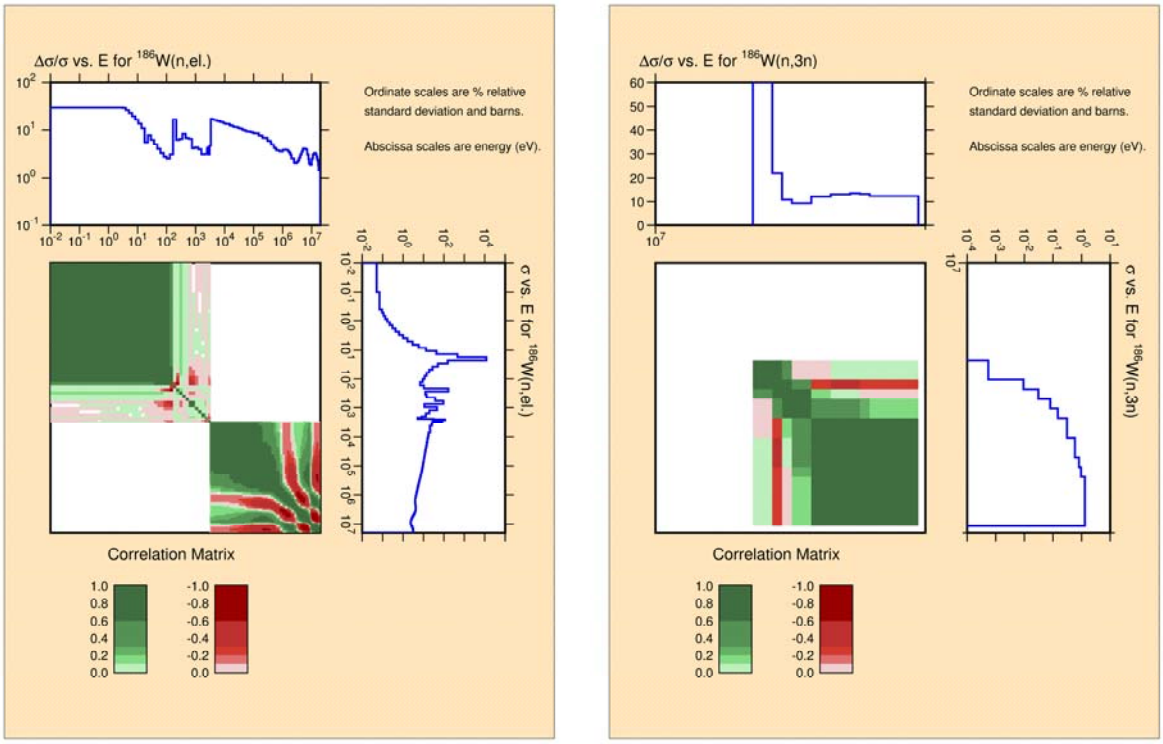

Fig.61 Example of covariance matrices calculated for elastic cross-section and (n,3n) cross-section for ^{186}W. Plots were prepared using the NJOY code.

Acknowledgement

This work has been carried out within the framework of the EUROfusion Consortium and has received funding from the Euratom research and training programme 2014-2018 and 2019-2020 under grant agreement No 633053. The views and opinions expressed herein do not necessarily reflect those of the European Commission.

References

[1] E. Bernard, R. Sakamoto, A. Kreter, M.F. Barthe, E.Autissier, P. Desgardin, H. Yamada, S. Garcia-Argote, G. Pieters, J. Chêne, B. Rousseau, C. Grisolia, Tungsten as a plasma-facing material in fusion devices: impact of helium high-temperature irradiation on hydrogen retention and damages in the material, *Physica Scripta* 2017, T170 (2017) 014023

[2] P. Pereslavtsev, U. Fischer, Evaluation of n+W cross section data up to 150 MeV neutron energy, AIP Conference Proceedings 769 (2005) 215; https://doi.org/10.1063/1.1944993

[3] The Joint Evaluated Fission and Fusion File. JEFF-3.3, http://www.oecd-nea.org/dbdata/jeff/jeff33/index.html

[4] A.J. Koning, S. Hilaire and M.C. Duijvestijn, TALYS-1.0, Proc. International Conference on Nuclear Data for Science and Technology, April 22-27, 2007, Nice, France, editors O. Bersillon, F. Gunsing, E. Bauge, R. Jacqmin, and S. Leray, EDP Sciences, 2008, p. 211

[5] A.J. Koning, S. Hilaire, M. Duijvestijn, TALYS-1.7, A nuclear reaction program, Nuclear Research and Consultancy Group (NRG), May 7, 2015

[6] A.Yu. Konobeyev, U. Fischer, A.J. Koning, P.E. Pereslavtsev, M. Blann, Implementation of the geometry dependent hybrid model in TALYS, *J. Korean Physical Society* 59 (2011) 935

[7] A.Yu. Konobeyev, U. Fischer, P.E. Pereslavtsev, A. Koning, M. Blann, Implementation of GDH model in TALYS-1.7 code, KIT Scientific Working Papers 45, 2016

[8] M. Blann, Importance of the nuclear density distribution on pre-equilibrium decay, *Phys. Rev. Lett.* 28 (1972) 757

[9] M. Blann, H.K. Vonach, Global test of modified precompound decay models, *Phys. Rev. C* 28 (1983) 1475

[10] M. Blann, ALICE-91: Statistical model code system with fission competition, RSIC Code Package PSR-146, 1991

[11] C.H.M. Broeders, A.Yu. Konobeyev, A.Yu. Korovin, V.P. Lunev, M. Blann, ALICE/ASH - Pre-compound and evaporation model code system for calculation of excitation functions, energy and angular distributions of emitted particles in nuclear reactions at intermediate energies, Report FZKA 7183, May, 2006, http://bibliothek.fzk.de/zb/berichte/FZKA7183.pdf

[12] ENDF-6 formats manual, Report BNL-90365-2009 Rev.2, Ed. A. Trkov, M. Herman and D. A. Brown, October 24, 2012

[13] J. Raynal, ECIS-06: Code system to solve coupled differential equations arising in nuclear model calculations, RSICC PSR-227, 2007

[14] W. Hauser, H. Feshbach, The inelastic scattering of neutrons, *Phys. Rev.* 87 (1952) 366

[15] A.V. Ignatyuk, G.N. Smirenkin, A.S. Tishin, Phenomenological description of the energy dependence of the level density parameter, *Sov. J. Nucl. Phys.* 21 (1975) 255

[16] A. Gilbert, A.G.W. Cameron, A composite nuclear-level density formula with shell corrections, *Can. J. Phys.* 43 (1965) 1446

[17] D. L. Smith, Covariance matrices for nuclear cross sections derived from nuclear model calculations, ANL/NDM-159, Argonne National Laboratory, 2004

[18] A.J. Koning and D. Rochman, Modern nuclear data evaluation with the TALYS code system, *Nucl. Data Sheets* 113 (2012) 2841

[19] A.J. Koning, TEFAL-1.9: Making nuclear data libraries using TALYS, Nuclear Research and Consultancy Group (NRG), November 2017

[20] L.E. Beghian, H.H. Halban, Absolute cross-sections for the capture of neutrons of 200 and 900 keV energy, *Nature* 63 (1949) 366

[21] M. Bhike, B.J. Roy, A. Saxena, R.K. Choudhury, S. Ganesan, Measurement of ^{232}Th(n,γ)^{233}Th, ^{98}Mo(n,γ)^{99}Mo, ^{186}W(n,γ)^{187}W, ^{115}In(n,γ)^{116m1}In, and ^{92}Mo(n,p) ^{92m}Nb cross sections in the energy range of 1.6 to 3.7 MeV, *Nucl. Sci. Eng.* 170 (2012) 44

[22] M.V. Bokhovko, L.E. Kazakov, V.N. Kononov, E.D. Poletaev, V.M. Timokhov, A.A. Voevodskiy, The measurement of the neutron capture cross-section for tungsten isotopes in the energy range from 5 to 400 keV, *Yadernaya Fizika* 46 (1987) 51, Engl. translation: *Soviet Journal of Nuclear Physics* 46 (1987) 33

[23] R.F. Coleman, B.E. Hawker, L.P. O'Connor, J.L. Perkin, Cross sections for (n,p) and (n,alpha) reactions with 14.5 MeV neutrons, Proceedings of the Physical Society (London), 73 (1959) 215

[24] M. Dikšić, P. Strohal, G. Pető, P. Bornemisza-Pauspertl, I. Hunyadi, J. Károlyi, Additional measurements of the radiative capture cross sections for 3 MeV neutrons, *Acta Physica Academiae Scientiarum Hungaricae* 28 (1970) 257

[25] F.S. Dietrich, J.D. Anderson, R.W. Bauer, S.M. Grimes, R.W. Finlay, W.P. Abfalterer, F.B. Bateman, R.C. Haight, G.L. Morgan, E. Bauge, J.P. Delaroche, P. Romain, Importance of isovector effects in reproducing neutron total cross section differences in the W isotopes, *Phys. Rev. C* 67 (2003) 044606

[26] W. Dilg, H. Vonach, G. Winkler, P. Hille, Measurement of (n,2n) reactions cross-sections on heavy nuclei, *Nuclear Physics A* 118 (1968) 9

[27] A.A. Druzhinin, A.A. Lbov, L.P. Bilibin, Cross-section of the reactions W186(n,2n)W185, W184(n,g)W185, and W186(n,g)W187 for fission neutrons and W186(n,2)W185 and W182(n,2n)W181 For 14.8 MeV neutrons, *Yadernaya Fizika* 4 (1966) 515, Engl. translation: *Soviet Journal of Nuclear Physics* 4 (1967) 366

[28] A.N. Djumin, A.I. Egorov, V.M. Lebedev, G.N. Popova, V.A.Smolin, Nuclear radii for some isotopes derived from total neutron cross-sections, Conf: 4.All Union Conf. on Neutron Phys., 18-22 Apr 1977, Kiev, Vol.2, (1977) p.74

[29] A.A. Filatenkov, Neutron activation cross sections measured at KRI in neutron energy region 13.4 - 14.9 MeV, INDC(CCP)-0460, 2016

[30] A.A. Filatenkov, S.V. Chuvaev, Experimental determination of cross sections for several insufficiently known neutron induced reaction on heavy nuclei (Z=74-79), Khlopin Radiev. Inst. RI-259, 2003

[31] D.G. Foster, Jr., D.W. Glasgow, Neutron total cross sections, 2.5 - 15 MeV. I. Experimental, *Phys. Rev. C* 3 (1971) 576

[32] J. Frehaut, A. Bertin, R. Bois, J.Jary, G. Mosinski, Status of (n,2n) cross section measurements at Bruyeres-le-Chatel, INDC(USA)-84,(1), p.399, 1980, Revised data: Report CEA-R-6447, 2016

[33] A. Grallert, J. Csikai, Cs.M. Buczko, I. Shaddad, Investigations on the systematics in (n,α) cross sections at 14.6 MeV INDC(NDS)-286, p.131, 1993

[34] P.T. Guenther, A.B. Smith, J.F. Whalen, Fast-neutron total and scattering cross sections of ^{182}W, ^{184}W, and ^{186}W, *Phys. Rev.* C 26 (1982) 2433

[35] Guohui Zhang, Zhaomin Shi, Guoyou Tang, Jinxiang Chen, Guangzhi Liu, Hanlin Lu, Interference of the low-energy neutrons on activation cross-section measurement of the ^{186}W(n,γ)^{187}W reaction, *Nucl. Sci. Eng.* 137 (2001) 107

[36] D. Hermsdorf, A. Meister, S. Sassonoff, D. Seeliger, K. Seidel, Integrated data from measurement of absolute differential neutron emission cross-section at 14 MeV incident neutron energy, Priv. Comm (EXFOR): Hermsdorf (1982), EXFOR: 30397028

[37] D. Hermsdorf, S. Sassonoff, D. Seeliger, K. Seidel, Absolute differentielle Neutronenemissionsquerschnitte für Ti, V und Cr bei 14 MeV Einschussenergie, *Kernenergie* 17 (1974) 176

[38] Y. Ikeda, C. Konno, A. Kumar, Y. Kasugai, Summary of activation cross sections measurements at FNS, INDC(NDS)-342, p.19, 1996

[39] Y. Ikeda, C. Konno, K. Oishi, T. Nakamura, H. Miyade, K. Kawade, H. Yamamoto, T. Katoh, Activation cross section measurements for fusion reactor structural materials at neutron energy from 13.3 to 15.0 MeV using FNS facility, JAERI-1312, 1988

[40] A.E. Johnsrud, M.G. Silbert, H.H. Barschall, Energy dependence of fast-neutron activation cross sections, *Phys. Rev.* 116 (1959) 927

[41] Kaihong Fang, Shiwei Xu, Changlin Lan, Xiaosan Xu, Xiangzhong Konga, Rong Liu, Li Jiang Cross-section measurement for the reactions producing short-lived nuclei induced by neutrons around 14 MeV, *Applied Radiation and Isotopes* 66 (2008) 1104

[42] H.C. Kao, D.L. Humphrey, The (n,2n) isomeric cross sections for ^{87}Rb, ^{112}Cd, ^{138}Ba, and ^{186}W, *Bulletin of the American Physical Society* 19 (1974) p.700 (EC7)

[43] Y. Kasugai, M. Asai, A. Tanaka, H. Yamamoto, I. Jun, T. Iida, K. Kawade, Measurement of activation cross sections on tantalum and tungsten with 14 MeV neutrons, *J. Nuclear Science and Technology* 31 (1994) 1248

[44] Y. Kasugai, H. Yamamoto, A. Takahashi, T. Iida, K. Kawade, Measurements of activation cross sections on Ta, W for 14 MeV neutrons, JAERI-M-93-046, p.277,1993

[45] G.D. Kim, H.J. Woo, H.W. Choi, N.B. Kim, T.K. Yang, J.H. Chang, K.S. Park, Measurements of fast neutron capture cross sections on ^{63}Cu and ^{186}W, *Journal of Radioanalytical and Nuclear Chemistry* 271 (2007) 553

[46] K. Knopf, W. Waschkowski, INteraction of neutrons with tungsten and its isotopes, *Zeitschrift für Naturforschung A* 42 (1987) 909

[47] Kong Xiangzhong, Hu Shangbin, Yang Jingkang, Cross sections of 14 MeV neutron induced reactions on wolfram isotopes, INDC(CPR)-042, p.9, 1997

[48] V.N. Kononov, Yu.Ya. Stavisskii, V.E. Kolesov, A.G. Dovbenko, S. Nesterenko, V.I. Moroka, Radiative capture cross sections of 30-170 keV neutrons, Rept: Fiz.-Energ Institut, Obninsk, 29 1965

[49] A.I. Leipunskiy, O.D. Kazachkovskiy, G.Ja. Artyukhov, A.I. Baryshnikov, T.S. Belanova, V.I. Galkov, Yu.Ja. Stavisskiy, E.A. Stumbur, L.E. Sherman, Radiative capture cross-section measurements for fast neutrons, Second Internat. At. En. Conf., Geneva 1958, Vol.15 (1958) p.50 (2219)

[50] M. Lindner, J. Miskel, Miscellaneous neutron reaction cross sections, Washington AEC Office Reports, No.1018 (1959) p.63

[51] M. Lindner, R.J. Nagle, J.H. Landrum, Neutron capture cross-sections from 0.1 to 3 MeV by activation measurements, *Nucl. Sci. Eng.* 59 (1976) 381

[52] D. Lister, A.B. Smith, C. Dunford, Fast-neutron scattering from the 182, 184, and 186 isotopes of tungsten, *Phys. Rev.* 162 (1967) 1077

[53] Lu Hanlin, Zhao Wenrong, Yu Weixiang, Cross-section measurement for reactions Ba-137(n,p)Cs-137, W-182(n,nalpha)Hf-178m2 and Ir-193(n,2n)Ir-192m2 at 14 MeV, *Chinese J. of Nuclear Physics (Beijing)* 16 (1994) 267

[54] A.A. Lychagin, S.P. Simakov, B.V. Devkin, B.V. Zhuravlev, M.G. Kobosev, O.A. Salnikov, V.A. Talalaev, T. Sztaricskai, Neutron spectra from 52Cr(N,N`G) and 208Pb(N,N`G) reactions at an incident neutron energy of 14.1 MeV, Symp. on Nucleon Induced Reactions, Smolenice 1988, p.272

[55] W.S. Lyon, R.L. Macklin, Neutron activation at 195 keV, *Phys. Rev.* 114 (1959) 1619

[56] R.L. Macklin, D.M. Drake, E.D. Arthur Neutron capture cross sections of ^{182}W, ^{183}W, ^{184}W, and ^{186}W from 2.6 to 2000 keV, *Nucl. Sci. Eng.* 84 (1983) 98

[57] G. Magnusson, P. Andersson, I. Bergqvist, 14.7 MeV Neutron capture cross-section measurements with activation technique, *Physica Scripta* 21 (1980) 21.

[58] R.C. Martin, P.F. Yergin, R.H. Augustson, N.N. Kaushal, H.A. Medicus, E.J. Winhold, MeV neutron total cross sections of Ta and W isotopes, *Bulletin of the American Physical Society* 12 (1967) p.106 (GD12)

[59] G.N. Maslov, F.Nasyrov, N.F.Pashkin, Experimental cross-sections for nuclear reactions involving neutrons with energies of about 14 MeV, INDC(CCP)-42, p.50, 1974, English transl. of *Jadernye Konstanty* 9 1972

[60] S. Matsuyama, T. Okubo, M. Baba, T. Ito, T. Akiyama, N. Ito, N. Hirakawa, Measurement of double-differential neutron emission cross sections of Mo, Ta and W, JAERI-M Reports, No.93-046, 1992, p.345

[61] J.A. Miskel, K.V. Marsh, M. Lindner, R.J. Nagle, Neutron activation cross sections, *Phys. Rev.* 128 (1962) 2717

[62] S.K. Mukherjee, H. Bakhru, Some (n,alpha) reaction cross-sections and the resulting radio-isotopes, Conf: Nucl.and Sol. State Physics Symp., Bombay 1963, p.244

[63] S. Murahira, Y. Satoh, N. Honda, A. Takahashi, T. Iida, M. Shibata, H. Yamamoto, K. Kawade, Measurement of formation cross sections producing short-lived nuclei by 14 MeV neutrons - Pr, Ba, Ce, Sm, W, Sn, Hf, INDC(JPN)-175, p. 171, 1996

[64] M.V. Pasechnik, I.F. Barchuk, I.A.Totskiy, V.I. Strizhak, A.M. Korolev, Yu.V. Gofman, G.N. Lovchikova, E.A. Koltypin, G.B. Yan`kov, Scattering and capture of fast neutrons by the nuclei, Second Internat. At. En. Conf., Geneva 1958, Vol.15, p.18

[65] J.L. Perkin, L.P. O`Connor, R.F. Coleman, Radiative capture cross sections for 14.5 MeV neutrons, Proceedings of the Physical Society (London), Vol.72, (1958 p.505

[66] A. Poularikas, R.W. Fink, D.G. Gardner, Absolute activation cross-sections for 14.8 neutrons, Univ. of Arkansas Reports, No.59, 1960, p.4

[67] R. Prasad, D.C. Sarkar, C.S. Khurana, Measurement of (n,2n) reaction cross sections at 14.8 MeV, *Nucl. Phys.* 88 (1966) 349

[68] S.M. Qaim, C. Graca, Neutron activation cross sections at 14.7 MeV for isotopes of tungsten, *Nuclear Physics A* 242 (1975) 317

[69] E. Rurarz, J. Chwaszczewska, Z. Haratym, M. Pietrzykowski, A. Sulik, Excitation of isomeric activities in Rb, Y, Pd, Cd, W, Os and Pb using 14.8 MeV neutrons, *Acta Physica Polonica, Part B* 2 (1971) 553

[70] H.Sakane, Y.Kasugai, M.Shibata, H.Takeuchi, K.Kawade, Measurements of the (n, np+d) activation cross sections with 13.4-14.9 MeV neutrons using a fusion neutronics source/JAERI, *Annals of Nuclear Energy* 30 (2003) 1847

[71] H. Sakane, M. Shibata, K. Kawade, Y. Kasugai, Y. Ikeda, Systematic (n,np) Reaction cross sections by 14 MeV neutrons, JAERI Conference proceedings, No.2000-005, 1999, p.202,

[72] D. Schmidt, W. Mannhart, S. Khurana, Determination of differential elastic and double-differential neutron scattering cross sections of elemental tungsten at energies between 7.19 MeV and 14.10 MeV, Phys. Techn. Bundesanst., Neutronenphysik Reports, No.51, 2006

[73] O. Schwerer, M. Winkler-Rohatsch, H. Warhanek, G. Winkler, Measurement of cross sections for 14 MeV neutron capture, *Nucl. Phys. A* 264 (1976) 105

[74] S.P. Simakov, B.V. Devkin, M.G. Kobosev, A.A. Lychagin, V.A. Talalaev, C. Sandin, Differential neutron emission cross-sections for beryllium and tangsten at 14 MeV incident neutron energy, INDC(NDS)-272, (131), 1992

[75] W. Selove, Resonance-region neutron spectrometer measurements on silver and tungsten, *Phys. Rev.* 84 (1951) 869

[76] V. Semkova, R. Capote, R.J. Tornin, A.J. Koning, A. Moens, A.J.M. Plompen, New cross section measurements for neutron-induced reactions on Cr, Ni, Cu, Ta and W isotopes obtained with the activation technique Conf. on Nucl.Data for Sci. and Technology, Nice 2007, Vol.1, p.559, 2007

[77] Yu.Ya. Stavisskii, V.A. Tolstikov, Fast neutron radiative capture cross sections of V-51, NB-93, W-186 and TL-205, *Atomnaya Energiya* 9, Issue.5 (1960) 869, *Soviet Atomic Energy* 9 (1961) 942

[78] A. Takahashi, Y. Sasaki, H. Sugimoto, Measurement and analysis of double differential neutron emission cross sections at En = 14.1 MeV for 93Nb and 181Ta, Osaka Univ., Oktavian Reports, No.92-01, 1992

[79] Yu.N. Trofimov, Neutron radiation capture cross-sections for nuclei of medium and large masses at the neutron energy 1 MeV, Conf: 1. Int .Conf. on Neutron Physics, 14-18 Sep 1987 Kiev, Vol.3, p.331

[80] M. Valkonen, P. Homberg, R. Rieppo, J.K. Keinaenen, J. Kantele, Studies of 14 MeV neutron activation cross sections with special reference to the capture reaction, Rept: Univ. of Jyvaeskylae, Dept. of Physics, No.1/1976, 1976

[81] J. Voignier, S. Joly, G. Grenier, Neutron capture cross section measurements of rubidium, yttrium, niobium, gadolinium, tungsten, platinum and thallium between 0.5 and 3.0 MeV, CEA-R-5089, 1981

[82] H. Vonach, A. Chalupka, F. Wenninger, G. Staffel, Measurement of the angle-integrated secondary neutron spectra from interaction of 14 MeV neutrons with medium and heavy nuclei, INDC(USA)-84,(1), p.343, 1980

[83] Vuong Huu Tan, Nguyen Canh Hai, Pham Ngoc Son, Tran Tuan Anh, Neutron capture cross section measurements of ^{109}Ag, ^{186}W and ^{158}Gd on filtered neutron beams of 55 and 144 keV, INDC(VN)-011, 2004

[84] J.F. Whalen, J.W. Meadows, Fast neutron total cross sections using a mono-energetic source and an automated facility., Argonne National Laboratory report series, No.7210, p.16, 1966

[85] G.G. Zaikin, I.A. Korzh, N.T. Sklyar, I.A. Totskii, Cross sections for radiative capture of fast neutrons by Cu-63, Cu-65, W-186 isotopes, *Soviet Atomic Energy* 25 (1968) 1362, translation of *Atomnaya Energiya* 25, Issue.6, (1968) 526

[86] Experimental Nuclear Reaction Data (EXFOR), https://www-nds.iaea.org/exfor/exfor.htm

[87] D.E. Cullen, A. Trkov, Computational format C4, https://www-nds.iaea.org/nrdc/basics/exfor-basics-3.html#Computational_Format_C4

[88] ENSDF: Evaluated Nuclear Structure Data File Search and Retrieval, https://www. nndc.bnl.gov/ensdf/EnsdfDispatcherServlet

[89] D.L. Smith, A Least-squares computational tool kit, ANL/NDM-128, Argonne National Laboratory, 1993

[90] A.Yu. Konobeyev, U. Fischer, P.E. Pereslavtsev, Computational approach for evaluation of nuclear data including covariance information, *J. Kor. Phys. Soc.* 59 (2011) 923.

[91] The NJOY Nuclear data processing system, version 2016, https://www.njoy21.io/NJOY2016/

[92] ENDF-6 Checking & Utility Codes, https://www-nds.iaea.org/public/endf/utility/

[93] A. Trkov, Program COVEIG, https://www-nds.iaea.org/IRDFF/coveig.for

[94] J.-Ch. Sublet, L.W. Packer, J. Kopecky, R.A. Forrest, A.J. Koning, D.A. Rochman, The European Activation File: EAF-2010 neutron-induced cross section library, EASY Documentation Series CCFE-R (10) 05, 2010, http://www.ccfe.ac.uk/EASY-data/eaf2010/Docs/EAF_n_Cross_sections_2010.pdf

[95] K. Shibata, O. Iwamoto, T. Nakagawa, N. Iwamoto, A. Ichihara, S. Kunieda, S. Chiba, K. Furutaka, N. Otuka, T. Ohsawa, T. Murata, H. Matsunobu, A. Zukeran, S. Kamada, J. Katakura: JENDL-4.0: A new library for Nucl. Sci. Eng., *J. Nucl. Sci. Technol.* 48(1) (2011) 1, https://wwwndc.jaea.go.jp/jendl/j40/update/

[96] JENDL-4.0 High Energy File (JENDL-4.0/HE), https://wwwndc.jaea.go.jp/ftpnd/jendl/jendl40he.html

[97] JENDL Activation Cross Section File for Nuclear Decommissioning 2017 (JENDL/AD-2017), https://wwwndc.jaea.go.jp/ftpnd/jendl/jendl-ad-2017.html

[98] JENDL High Energy File 2007 (JENDL/HE-2007), https://wwwndc.jaea.go.jp/ftpnd/jendl/jendl-he-2007.html

[99] D.A. Brown, M.B. Chadwick, R. Capote, A.C. Kahler, A. Trkov, M.W. Herman, A.A. Sonzogni, Y. Danon, A.D. Carlson, M. Dunn, D.L. Smith, G.M. Hale, G. Arbanas, R. Arcilla, C.R. Bates, B. Beck, B. Becker, F. Brown, R.J. Casperson, J. Conlin, D.E. Cullen, M.-A. Descalle, R. Firestone, T. Gaines, K.H. Guber, A.I. Hawari, J. Holmes, T.D. Johnson, T. Kawano, B.C. Kiedrowski, A.J. Koning, S. Kopecky, L. Leal, J.P. Lestone, C. Lubitz, J.I. Márquez Damián, C.M. Mattoon, E.A. McCutchan, S. Mughabghab, P. Navratil, D. Neudecker, G.P.A. Nobre, G. Noguere, M. Paris, M.T. Pigni, A.J. Plompen, B. Pritychenko, V.G. Pronyaev, D. Roubtsov, D. Rochman, P. Romano, P. Schillebeeckx, S. Simakov, M. Sin, I. Sirakov, B. Sleaford, V. Sobes, E.S. Soukhovitskii, I. Stetcu, P. Talou, I. Thompson, S. van der Marck, L. Welser-Sherrill, D. Wiarda, M. White, J.L. Wormald, R.Q. Wright, M. Zerkle, G. Žerovnik, Y. Zhu, ENDF/B-VIII.0: The 8th major release of the nuclear reaction data library with cielo-project cross sections, new standards and thermal scattering data, *Nuclear Data Sheets,* 148 (2018) 1; ENDF/B-VIII.0 (2018), http://www.nndc.bnl.gov/endf/b8.0/

[100] TALYS-based evaluated nuclear data library, TENDL-2017, https://tendl.web.psi.ch/tendl_2017/tendl2017.html

[101] V.S. Barashenkov, B.F. Kostenko, A.M. Zadorogny, Time-dependent intranuclear cascade model*, Nucl. Phys. A* 338 (1980) 413

[102] V.S. Barashenkov, Monte Carlo simulation of ionization and nuclear processes initiated by hadron and ion beams in media, *Comp. Phys. Comm.* 126 (2000) 28

[103] S.G. Mashnik, A.J. Sierk, CEM03.03 user manual, LA-UR-12-01364, (2012)

[104] S.G. Mashnik, L.M. Kerby, MCNP6 simulation of light and medium nuclei fragmentation at intermediate energies, EPJ Web of Conferences 117 (2016) 03008, https://doi.org/10.1051/epjconf/201611703008

[105] A.Yu. Konobeyev, U. Fischer, Reference data for evaluation of gas production cross-sections in proton induced reactions at intermediate energies, KIT SR 7660, 2014, http://goo.gl/26Vjzl ; www.ksp.kit.edu/download/1000038463

[106] A.Yu. Konobeyev, U. Fischer, Complete gas production data library for nuclides from Mg to Bi at neutron incident energies up to 200 MeV, Report KIT SWP 36, 2015; http://goo.gl/F8hKLN ; http://digbib.ubka.uni-karlsruhe.de/volltexte/1000049466

KIT Scientific Working Papers
ISSN 2194-1629

www.kit.edu